

# Sustainable Food Technology

Accepted Manuscript

This article can be cited before page numbers have been issued, to do this please use: T. P. Vo, M. T. Nguyen, T. A. Nguyen, G. V. Nguyen, H. N. Nguyen, G. B. Pham, M. H. Ha and Q. D. Nguyen, *Sustainable Food Technol.*, 2025, DOI: 10.1039/D5FB00536A.



This is an Accepted Manuscript, which has been through the Royal Society of Chemistry peer review process and has been accepted for publication.

Accepted Manuscripts are published online shortly after acceptance, before technical editing, formatting and proof reading. Using this free service, authors can make their results available to the community, in citable form, before we publish the edited article. We will replace this Accepted Manuscript with the edited and formatted Advance Article as soon as it is available.

You can find more information about Accepted Manuscripts in the [Information for Authors](#).

Please note that technical editing may introduce minor changes to the text and/or graphics, which may alter content. The journal's standard [Terms & Conditions](#) and the [Ethical guidelines](#) still apply. In no event shall the Royal Society of Chemistry be held responsible for any errors or omissions in this Accepted Manuscript or any consequences arising from the use of any information it contains.



Microwave-enzymatic-assisted extraction is a combination of green technology with great potential in enhancing the extraction yield of bioactive compounds from plants, such as *Coriandrum sativum* L. leaves. Natural deep eutectic solvents are green solvents synthesized by combining organic acid and choline chloride from living organisms' cells. The combination of microwave-enzymatic-assisted extraction and natural deep eutectic solvents makes way for the development of sustainable food processing objectives. Microwave-enzymatic-assisted extraction provided rapid heating and hydrolysis of rigid plant cell walls. This combination significantly improves bioactive compounds' extraction yield without deterioration, which usually happens with conventional extraction techniques. Through natural deep eutectic solvents characterization, this work explains how different types of natural deep eutectic solvents affect the recovery yield of bioactive compounds from *Coriandrum sativum* L. leaves. This study also describes the mechanisms of the combined technology based on the support of thermodynamic modeling, scanning electron microscopy, and X-ray diffraction. Results show that careful control of parameters like microwave power and enzyme activity is essential in achieving maximum efficiency without compromising the product quality. This study highlights the technological advantages of Microwave-enzymatic-assisted extraction while supporting its potential for broader adoption as a sustainable, bioactive compound-preserving approach in food supply chains. Moreover, it underscores the role of regional biodiversity in driving the development of innovative food products that contribute to human health and environmental sustainability.



1 **Improving the recovery of phenolics and flavonoids from *Coriandrum sativum***  
2 **L. leaves using microwave-enzymatic-assisted extraction.**

3 Tan Phat Vo<sup>1,2</sup>, Minh Thu Nguyen<sup>1,2</sup>, Thuy Anh Nguyen<sup>1,2</sup>, Gia Vinh Nguyen<sup>1,2</sup>, Hoang Nhan  
4 Nguyen<sup>1,2</sup>, Gia Bao Pham<sup>1,2</sup>, Minh Hoa Ha<sup>1,2\*</sup>, Dinh Quan Nguyen<sup>1,2\*</sup>

5 <sup>1</sup>Laboratory of Biofuel and Biomass Research, Faculty of Chemical Engineering, Ho Chi Minh  
6 City University of Technology (HCMUT), 268 Ly Thuong Kiet Street, District 10, Ho Chi Minh  
7 City, Vietnam

8 <sup>2</sup>Vietnam National University Ho Chi Minh City, Linh Trung Ward, Thu Duc City, Ho Chi Minh  
9 City, Vietnam

10 \*Corresponding author: [ndquan@hcmut.edu.vn](mailto:ndquan@hcmut.edu.vn) (Dinh Quan Nguyen),  
11 [hoa.ha169@hcmut.edu.vn](mailto:hoa.ha169@hcmut.edu.vn) (Minh Hoa Ha)

12 **Abstract**

13 This study focused on optimizing the extraction of phenolic compounds and flavonoids from  
14 leaves of *Coriandrum sativum* L. using a sequential green extraction approach based on  
15 microwave-enzymatic-assisted extraction (MEAE). Utilizing the Glycerol and Choline Chloride  
16 solvent system (composed of Gly - Cho in a molar ratio of 2:1, with water), several extraction  
17 parameters were systematically investigated for their influence on total phenolic content (TPC)  
18 and total flavonoid content (TFC): solid-to-liquid ratio, water content, microwave power,  
19 microwave time, enzyme concentration, and enzyme incubation time. Subsequent optimization  
20 established the following conditions: a solid-to-liquid ratio of 1/20 g/mL, 10% water content in  
21 solvent, 1022 W microwave power, 2.6 minutes microwave time, 40 U/g enzyme concentration,  
22 and 90 minutes enzyme incubation time at 50 °C. Under these optimized parameters, the TPC of  
23 the extracts reached 18.15 mg GAE/g, while the TFC optimized parameters reached 26.36 mg  
24 RE/g. The significance of variables was evaluated using Plackett–Burman Design, while optimal  
25 conditions were determined via Box-Behnken Design. Furthermore, the extraction kinetics were  
26 modeled using a second-order kinetic model to understand the mechanism. The findings  
27 demonstrate that the sequential MEAE technique, optimized via statistical and kinetic models,  
28 holds significant promise as an effective green method for enhancing the recovery of antioxidant  
29 compounds from *Coriandrum sativum* L.

30 **Keywords:** phenolics, flavonoids, natural deep eutectic solvent, microwave-enzyme-assisted  
31 extraction, coriander



## 32 1 Introduction

33 *Coriandrum sativum L.*, known as coriander or cilantro, is a popular cultivated herb in cuisines  
34 and traditional medical applications<sup>1</sup>. Native to the Mediterranean and Southwest Asia, it is now  
35 extensively grown in regions such as India, China, Egypt, Russia, and other tropical zones. In  
36 traditional medicine, coriander supports digestive health and alleviates symptoms including  
37 bloating, nausea, and diarrhea. It is also used in the treatment of urinary tract disorders,  
38 inflammation, anxiety, and insomnia. Coriander is high in bioactive compounds, especially  
39 antioxidants<sup>2</sup>. Significant amounts of flavonoids, carotenoids, and phenolic compounds – in  
40 particular, gallic acid, ferulic acid – have been found through quantitative analyses. These  
41 phenolics possess antioxidant capacity by scavenging free radicals, which is a significant  
42 contributor to the development of chronic diseases such as diabetes, cancer, heart disease, and  
43 neurological disorders. Additionally, these drugs support cardiovascular health by reducing blood  
44 pressure and low-density lipoprotein cholesterol. Iram Iqbal et al., (2023) stated that plant  
45 polyphenols can prevent atherosclerosis by regulating vascular endothelial function through the  
46 release of nitric oxide (NO) and reducing LDL oxidation to prevent atherosclerosis. Cardiovascular  
47 diseases, such as stroke, hypertension, and ischemic heart disease, can be prevented by dietary  
48 polyphenols<sup>3</sup>.

49 Extracting phenolic compounds from *Coriandrum sativum L.* is necessary to obtain beneficial  
50 active components, and the selection of solvent greatly influences the effectiveness of this process.  
51 Traditional solvents, such as methanol, ethanol, and acetone, are being gradually replaced by more  
52 environmentally friendly alternatives in the pursuit of sustainable and eco-friendly solutions.  
53 Natural Deep Eutectic Solvents (NDES) represent one such potential. NDES are an emerging class  
54 of solvents, typically formed from mixtures of two or more pure solid or liquid components<sup>4</sup>.  
55 When mixed in specific proportions, these components form a mixture with a melting point that is  
56 significantly lower than that of each pure component.

57 This low melting point is typically below room temperature, rendering the mixture a liquid at  
58 room temperature. NDES are distinguished by several excellent properties, making them an  
59 attractive choice for extracting natural compounds. One of the most important is their low melting  
60 point, which allows them to exist in a liquid state without needing much energy. In addition, NDES  
61 are highly regarded for their safety due to their low toxicity, non-volatile, and non-flammable  
62 properties, making them more environmentally and user-friendly than traditional organic solvents.  
63 The recyclability and reusability of many NDES help reduce waste and costs. Finally, the  
64 turnability properties allow scientists to change the composition to optimize solubility for each  
65 specific target compound. NDES is opening a new era of sustainable and efficient extraction  
66 methods<sup>4</sup>.



67 Traditional extraction procedures, such as maceration, Soxhlet extraction, and reflux, are  
68 inexpensive and straightforward; however, they can be time-consuming, solvent-intensive, and  
69 inefficient. Furthermore, prolonged exposure to heat during these operations can damage sensitive  
70 substances. To address these drawbacks, advanced extraction technologies have been developed  
71 to improve efficiency, reduce processing time and solvent use, and better preserve the bioactivity  
72 of target compounds <sup>5</sup>. Among these, Microwave-Assisted Extraction (MASE) and Enzyme-  
73 Assisted Extraction (EASE) are two prominent techniques. MASE utilizes microwave energy to  
74 rapidly heat and pressurize plant cells, causing them to rupture and release phenolic compounds <sup>6</sup>.  
75 EASE uses hydrolytic enzymes such as cellulases, hemicellulases, and pectinases to break down  
76 the plant cell wall matrix and release intracellular phenolics into the solvent. While both MASE  
77 and EASE provide considerable advantages over traditional approaches, combining the two has  
78 emerged as a promising strategy. Microwaves are first used in this combined method to break  
79 down the structures and speed up the diffusion of phenolic compounds into the NDES solvent. The  
80 enzyme is then used to weaken further or break down the cell wall.

81 A comparative study determined MASE's effectiveness in isolating quercetin 3-O-glucoside, a  
82 bioactive compound with anti-diabetic properties, from *Gynura procumbens* <sup>6</sup>. The MASE method  
83 demonstrated significant advantages over conventional Soxhlet extraction, requiring only 5  
84 minutes of extraction time compared to 3 hours, and yielding a higher amount of quercetin (1.60  
85 mg/g vs. 1.40 mg/g). A custom-designed temperature-controlled MASE system was developed to  
86 enhance extraction efficiency and prevent the thermal degradation of bioactive compounds. This  
87 system utilizes feedback from a temperature sensor to regulate microwave output, ensuring precise  
88 thermal control throughout the process. These findings confirm that MASE, particularly in terms  
89 of temperature regulation, is a highly efficient and viable technique for extracting thermally  
90 sensitive bioactive compounds <sup>6</sup>. A food-friendly enzyme-assisted extraction (EASE) method was  
91 created and refined by Mridusmita Chaliha et al. to extract bioactive substances from freeze-dried  
92 Kakadu plum puree. To optimize the yields of free ellagic acid (fEA), ascorbic acid, and phenolics,  
93 they ascertain the ideal parameters for solvent concentration, enzyme concentration, and extraction  
94 duration. With a yield of 51.3%, the study found that the best conditions for extracting fEA were  
95 1.5% (w/w) propylene glycol, 300 mg/L pectolytic enzyme, and a 15-hour extraction period <sup>7</sup>.  
96 While previous studies have applied either MASE or EASE individually, few have systematically  
97 optimized their integration or identified the factors influencing extraction efficiency. The kinetic  
98 behavior and underlying mechanisms of the combined process also remain insufficiently  
99 elucidated <sup>8</sup>.

100 Therefore, this study focuses on optimizing the integrated MASE-EASE process using NDES to  
101 enhance the extraction efficiency and improve the recovery of bioactive compounds from



102 *Coriandrum sativum* L. leaves. Various extraction parameters, including solid-to-liquid ratio,  
103 water content, microwave power, enzyme concentration, and incubation time, were systematically  
104 optimized using Plackett–Burman and Box–Behnken designs. The extraction kinetics were  
105 modeled using a second-order kinetic model to elucidate the mass transfer mechanism.  
106 Additionally, the reusability of the NDES solvent and the cost and energy efficiency of the  
107 optimized MEAE process were evaluated to assess its industrial feasibility.

## 108 2 Materials and Methods

### 109 2.1 Materials

110 We purchased *Coriandrum sativum* from Binh Dien Wholesale Market in Ho Chi Minh City,  
111 Vietnam (the producing region is the Mekong Delta). To enable water evaporation, they were kept  
112 in a laboratory drier (model: TR-240, Nabertherm, Zürich, Germany) for 48 hours at 50 °C. A  
113 dried coriander powder (DCP) was created by grinding dried leaves in a grinder (model: SM 450L,  
114 Harlow, UK). The final powder was kept in an airtight plastic container and stored at 25 °C in a  
115 dry place, without direct sunlight. This storage condition was chosen to maintain the stability of  
116 the bioactive compounds while also preventing moisture absorption and inhibiting microbial  
117 growth.

### 118 2.2 Chemicals

119 Chemicals used to prepare NDES: Glycerol was purchased from Duc Giang Chemicals Group.  
120 Jsc (Hanoi, Vietnam); Acetic Acid, Lactic Acid, and Citric Acid were purchased from Guangdong  
121 Guanghua Sci-Tech Co., Ltd (Guangdong, China); Choline Chloride was purchased from HiMedia  
122 Laboratories Pvt.Ltd (Nasik, India); Erythritol and 1,2-propanediol were purchased from Hoa Nam  
123 Chemicals – Laboratory Equipment Company, Ltd.

124 The following analytical reagents were used: aluminum chloride ( $AlCl_3$ ), sodium carbonate  
125 ( $Na_2CO_3$ ), sodium acetate ( $CH_3COONa$ ), ethanol (96%), and the Folin-Ciocalteu phenol reagent.  
126 Hoa Nam Chemicals – Laboratory Equipment Company, Ltd. (Ho Chi Minh City, Viet Nam) was  
127 the supplier of all chemicals.

### 128 2.3 Preparation for NDESs

129 To assess their phenolic and flavonoid extractability from DCP, fifteen distinct NDES were  
130 chosen, each with the same formulation and abbreviation shown in Table 1. A 2:1 molar ratio was  
131 applied to combine hydrogen bond donors (HBDs) and acceptors (HBAs). Then, a magnetic stirrer  
132 (model MS-H380-Pro, DLAB Scientific Co. Ltd., USA) was used to stir and heat the mixture to  
133 80 °C until it became transparent and homogenous. The solvents were acceptable for synthesis  
134 when they did not crystallize at room temperature.



135 The functional groups in NDES were analyzed using the Fourier Transform Infrared method,  
 136 following the previous study <sup>9</sup>. A drop of each NDES solvent was pipetted into the sample holder  
 137 of the PerkinElmer Spectrum 10.5.2 instrument (Model Frontier FT-IR/NIR 105667, USA), and  
 138 the spectrum was recorded within the 450-4000 cm<sup>-1</sup> range. The pH values of the NDES solvents  
 139 were measured using a pH meter (Model MI-151, Milwaukee, Romania, EU), while their densities  
 140 were determined through mass and volume measurements.

141 **Table 1.** Details of 15 synthesized NDESs

No.	Solvent	HBD	HBA	pH	Density (g/mL)
NDES1	Lac – Cho	Lactic acid	Choline chloride	0.97	1.156 ± 0.015h
NDES2	Lac – Gly	Lactic acid	Glycerol	0.60	1.186 ± 0.023fg
NDES3	Lac – Pro	Lactic acid	1,2-Propanediol	1.10	1.116 ± 0.014i
NDES4	Lac – Ery	Lactic acid	Erythritol	0.91	1.274 ± 0.006d
NDES5	Ci – Cho	Citric acid	Choline chloride	-0.52	1.384 ± 0.009c
NDES6	Ci – Gly	Citric acid	Glycerol	-0.72	1.414 ± 0.011b
NDES7	Ci – Pro	Citric acid	1,2-Propanediol	-1.67	1.444 ± 0.007a
NDES8	Ci – Ery	Citric acid	Erythritol	-1.59	1.434 ± 0.015ab
NDES9	Gly – Cho	Glycerol	Choline chloride	3.36	1.164 ± 0.008gh
NDES10	Pro – Cho	1,2-Propanediol	Choline chloride	3.14	1.234 ± 0.006e
NDES11	Ace – Cho	Acetic acid	Choline chloride	0.02	1.092 ± 0.015j
NDES12	Ace – Ery	Acetic acid	Erythritol	0.18	1.114 ± 0.020ij
NDES13	Ace – Gly	Acetic acid	Glycerol	-0.14	1.052 ± 0.008k
NDES14	Ace – Pro	Acetic acid	1,2-Propanediol	-0.84	1.032 ± 0.017k
NDES15	Ery – Cho	Erythritol	Choline chloride	2.47	1.206 ± 0.014f

142 \* The letters a, b ... and k represent statistically significant differences. Samples sharing the same  
 143 letters (e.g., fg and gh or a and ab) are not significantly different in density, while samples with  
 144 different letters are significantly different.



145           **2.4 Single-factor experiments of Microwave-assisted and Enzyme-assisted**  
146           **extraction**

147           In an amber glass vial, mix 10 mL of solvent with a precisely measured amount of DCP.  
148           Microwave radiation was applied to the mixture (model MOB-7733, TA RA Joint Stock  
149           Company, Vietnam). The experiment encompassed solid-to-liquid ratio (SLR) ranging from  
150           1/10, 1/20, 1/30, 1/40, 1/50, 1/60 g/mL, water content (WC) run from 0% to 50%, and specific  
151           microwave power (MP) settings of 0, 150, 300, 450, 600, 750 and 900 W applied for various  
152           microwave time (MT) 0.5, 1, 2, 3, and 4 minutes. Following microwave treatment, the samples  
153           were cooled to 50 °C. Different enzyme (EC) concentrations, ranging from 0 to 50 U/g, were  
154           added at 10 U intervals. A water bath (Model RS22L, 40 kHz, Rama Vietnam Joint Stock  
155           Company, Vietnam) was used for the enzymatic incubation at temperatures (EITem) of 50 °C  
156           for enzyme incubation times (EIT) of 30, 60, 90, 120, and 150 minutes. After incubation, the  
157           blend was filtered through filter paper to extract the bioactive compounds. The experiments of  
158           the single-factor are shown in Table S1.

159           **2.5 Quantification of bioactive compounds recovery**

160           **2.5.1 Total phenolic content (TPC)**

161           TPC was measured using the spectrophotometry method with minor changes <sup>10</sup>. 0.25 mL of  
162           diluted DCP sample was added to a test tube, followed by 0.25 mL of 10% (v/v) Folin &  
163           Ciocalteu's Reagent (0.19 N). After that, the sample was incubated in the dark for 5 minutes before  
164           adding 0.5 mL of 7.5% (w/v) Sodium Carbonate ( $\text{Na}_2\text{CO}_3$ ) and 4 mL of distilled water. The  
165           solution was left to react for 1 hour in a dark place at room temperature. The sample absorbance  
166           was measured using a UV-visible spectrophotometer (model: Cary 60, Agilent Technologies,  
167           USA) at an absorbance wavelength of 765 nm. TPC was expressed as milligrams of gallic acid  
168           equivalent per gram (mg GAE/g).

169           **2.5.2 Total flavonoid content (TFC)**

170           TFC was measured with minor changes using the spectrophotometry technique <sup>11</sup>. Disperse  
171           0.50 mL of diluted DCP sample into 1.00 mL of 96° ethanol. Then, add 0.10 mL of 1M potassium  
172           acetate ( $\text{CH}_3\text{COOK}$ ) solution, 0.10 mL of 10% aluminum trichloride solution ( $\text{AlCl}_3$ ), and 3.5 mL  
173           of distilled water. The mixtures were left in the dark room for half an hour. Using an absorbance  
174           wavelength of 415 nm, the sample absorbance was measured with a UV-visible spectrophotometer  
175           (model: Cary 60, Agilent Technologies, USA). Milligrams of rutin equivalent per gram (mg RE/g)  
176           was the unit of measurement used to express TFC.



177

## 2.6 Design of experiments

178

### 2.6.1 Plackett–Burman Design (PBD) model

179

In this study, the PBD was utilized to identify critical elements that significantly impact the extraction yields of DCP. PBD was selected for this study due to its efficiency in screening multiple variables with minimal experimental runs, requiring only 12 trials to assess six factors for each compound under investigation. Given that PBD focuses on main effects without considering interactions between factors, it is particularly suitable for estimating the individual contributions of each factor in the process, making it a valuable tool for preliminary screenings<sup>12</sup>. TPC and TFC were assessed as dependent responses, using "-1" and "+1" for the six tested components: solid-to-liquid-ratio (SLR), water content (WC), microwave power (MP), microwave time (MT), enzyme concentration (EC), and enzyme incubation time (EIT). With this standard, the baseline condition was set at "0", with "-1" denoting the lower level and "+1" the higher level. Equation (1) shows the relationship between the independent and dependent variables in the experiments.

190

$$y = \sum_{i=1}^n \beta_i x_i \quad (1)$$

191

Where  $x$  is the independent variable,  $y$  is the response variable;  $\beta$  is the regression coefficient; and  $i$  is the order of factors that were examined and how they affected the yield of each targeted compound;  $x_1, x_2, x_3, x_4, x_5, x_6$  are SLR, WC, MP, MT, EC, and EIT, respectively;  $y_1, y_2$  are phenolics and flavonoids, respectively;  $n$  is the number of factors examined ( $n = 6$ ). In the DCP extraction procedure, parameters with a p-value less than 0.05 significantly affected the yield of flavonoids and phenolics. The details of PBD are shown in Table S2.

197

### 2.6.2 Box-Behnken Design (BBD) model

198

The BBD enhanced the extraction process further once the PBD data were analyzed. Fourteen experimental runs, including two center points, were conducted to evaluate the connection between the response variables and specific independent variables. Equation (2) describes how the data were fitted to a second-order polynomial model:

202

$$y = \beta_0 + \sum_{i=0}^n \beta_i x_i + \sum_{i=0}^n \beta_{ii} x_i^2 + \sum_{i=0}^n \sum_{j=0}^n \beta_{ij} x_i x_j \quad (2)$$

203

Where  $y$  is the predicted response;  $\beta_0$  represents the intercept,  $\beta_i, \beta_{ii}, \beta_{ij}$  are the coefficients for linear, quadratic, and interaction terms, respectively. In this study, the dependent responses are defined as  $y_1$  for TFC expressed in (mg RE/g), and  $y_2$  for TPC expressed in (mg GAE/g). The



206 prediction error (%) between the experimental and predicted values was calculated according to  
207 Equation (3) to assess the model's accuracy:

$$208 \text{Prediction error} = \frac{\text{The mean of measured value} - \text{predicted value}}{\text{The mean of measured value}} \times 100 \quad (3)$$

## 209 2.7 Second-order extraction kinetic models

210 Second-order models were used to investigate the extraction kinetics of MEAE for recovering  
211 terpenoids and flavonoids from DCP. This model, which is based on Ho & McKay <sup>13</sup>, Equation  
212 (4) explains how quickly certain chemicals dissolve in solvents from powder:

$$213 \frac{dC_t}{dt} = \kappa (C_s - C_t)^2 \quad (4)$$

214 In the kinetic model,  $C_s$  denotes the equilibrium concentration of flavonoids or phenolic  
215 compounds (mg/g), while  $C_t$  represents their concentration at a given extraction time  $t$  (mg/g).  
216 The parameter  $\kappa$  indicates the second-order extraction rate constant (g/mg.min), whereas  $t$   
217 represents the extraction duration in minutes.

218 A linear Equation (5) is obtained by solving the differential equation (4) and rearranging:

$$219 \frac{t}{C_t} = \frac{t}{C_s} + \frac{1}{\kappa C_s^2} \text{ or } y = at + b \quad (5)$$

220 In this linear form:  $y$  corresponding to  $\frac{t}{C_t}$ ;  $a$  corresponding to  $\frac{1}{C_s}$ ;  $b$  corresponding to  $\frac{1}{\kappa C_s^2}$

221 When the extraction time  $t$  is zero, the initial extraction rate,  $\kappa$  (mg/min. g), is given by Equation  
222 (6):

$$223 \kappa = \kappa C_s^2 \quad (6)$$

224 Using Equation (5), the second-order extraction rate constant ( $\kappa$ ) is calculated by plotting  $\frac{t}{C_t}$   
225 versus  $t$ . Equation (7) is used to determine the Arrhenius constant ( $A_e$ , g/mg.min) and the activation  
226 energy ( $E_a$ , kJ/mol):

$$227 \ln \kappa = \ln A_e - \frac{A_e}{RT} \quad (7)$$

## 228 2.8 NDES recycle procedure

229 The reusability of the NDES9 was evaluated using AB-8 macroporous resin as an adsorbent, as  
230 described in a previous study <sup>14</sup>. Before use, the AB-8 resin was immersed in absolute ethanol for  
231 24 hours, and the AB-8 macroporous resin was thoroughly rinsed with ultrapure water to remove  
232 residual ethanol. It was stored in water until further use. First, NDES and DCP were mixed, then

233 the MEAE process was performed in optimized conditions. NDES extracts were passed through a  
234 glass chromatography column (20 cm bed height) packed with AB-8 resin at a flow rate of 1.0 bed  
235 volume (BV)·h<sup>-1</sup> at 25 °C. This allowed selective adsorption of phenolics and flavonoids onto the  
236 resin, while the NDES solvent was recovered in the effluent (NDES-reused). After adsorption, the  
237 column was first eluted with 70° ethanol to desorb phenolic/flavonoid compounds <sup>14</sup>. The NDES-  
238 reused was collected and reused directly in subsequent extraction cycles under the same MEAE  
239 conditions. The extraction efficiency (%) was determined as the ratio of the TPC and TFC yields  
240 obtained in each reuse cycle to those from the fresh solvent. Reusability of NDES was evaluated  
241 through 5 cycles <sup>15</sup>.

## 242 2.9 Cost and energy estimation

243 The economic and energy requirements of the optimized MEAE process were estimated on a 1  
244 L batch basis. The total operating cost ( $C_{total}$ ) was calculated as the sum of the energy  
245 consumption and solvent cost:

$$246 \quad C_{total} = C_{energy} + C_{solvent}$$

247 The total energy demand ( $E_{total}$ ) consisted of three main components, which are microwave  
248 heating, enzymatic incubation, and solvent evaporation.

$$249 \quad E_{total} = E_{microwave} + E_{incubation} + E_{evaporation}$$

250 Each term was calculated using:

$$251 \quad E = P \times t$$

252 Where  $P$  is the power rating of the equipment (kW) and  $t$  is the operation time (hour).

253 The energy required to heat or evaporate the solvent was additionally estimated using:

$$254 \quad Q = m \times C_p \times \Delta T$$

255 And

$$256 \quad Q_{evaporation} = m \times L_v$$

257 Where  $m$  is the solvent mass (kg),  $C_p$  is the specific heat capacity (kJ·kg<sup>-1</sup>·K<sup>-1</sup>),  $\Delta T$  is the  
258 temperature difference (K), and  $L_v$  is the latent heat of vaporization (kJ·kg<sup>-1</sup>).

259 The energy cost was then determined as:  $C_{energy} = E_{total} \times Electricity\ price$

260 The solvent cost was calculated from the mass of each chemical component in the NDES  
261 formulation:

$$262 \quad C_{solvent} = \sum m_i \times p_i$$



263 Where  $m_i$  is the mass (kg) and  $p_i$  is the market price ( $USD \cdot kg^{-1}$ ) of component  $i$   
264 The total operating cost per batch and cost per unit of extracted phenolic yield were compared  
265 between NDES-based and water-based extraction systems to evaluate process efficiency and  
266 scalability.

## 267 **2.10 Antioxidant Activity Determination**

268 Antioxidant activities were measured using a UV-visible spectrophotometer and a colorimetric  
269 method. Trolox was used as a reference to create standard calibration curves (0 – 40 mg TAE/g)  
270 to determine the results.

### 271 **2.10.1 ABTS**

272 Following a previously reported protocol, the ABTS radical scavenging experiment measured  
273 absorbance at 734 nm using a UV-visible spectrophotometer <sup>16</sup>. To make the ABTS<sup>+</sup> radical  
274 solution, 7.40 mM ABTS and 2.45 mM potassium persulfate were fully mixed in a 1:1 volume  
275 ratio and incubated for 18 hours at 25 °C in the dark. To assess the antioxidant activity, 3.90 mL  
276 of the resulting ABTS<sup>+</sup> solution and 0.10 mL of the diluted crude sample extract (CSE) were  
277 combined. A 20-minute dark incubation then preceded the spectrophotometric analysis. To express  
278 the results, the unit of measurement was Trolox equivalents per gram ( $\mu M$  TAE/g).

### 279 **2.10.2 DPPH**

280 A UV-visible spectrophotometer set to a detection wavelength of 515 nm was used to perform  
281 the DPPH radical scavenging experiment following a previously documented protocol <sup>17</sup>. In this  
282 experiment, 3.50 mL of ethanolic DPPH solution was mixed with 0.50 mL of the diluted crude  
283 sample extract (CSE). The mixture was then exposed to spectrophotometric analysis after being in  
284 the dark for 30 minutes. To express the results, the unit of measurement was Trolox equivalents  
285 per gram ( $\mu M$  TAE/g).

### 286 **2.10.3 Hydroxyl Radical**

287 Using a previously published technique, the hydroxyl radical ( $\cdot OH$ ) scavenging activity was  
288 assessed by measuring absorbance at 510 nm using UV-visible spectrophotometry <sup>18</sup>. Three stock  
289 solutions—8.8 mM hydrogen peroxide, 6 mM salicylic acid, and 9 mM ferrous sulfate ( $FeSO_4$ )—  
290 were prepared for the assay and mixed in a 2:5:5 volume ratio to create the reaction mixture. 2.4  
291 mL of the reaction mixture and 1.6 mL of the diluted CSE were combined for analysis, which was  
292 then spectrophotometrically examined after incubation in the dark for 15 minutes. The findings  
293 were presented as mg TAE/g, or  $\mu M$  Trolox equivalents per gram.



294 **2.10.4 FRAP**

295 A UV-visible spectrophotometer was used to quantify absorbance at 593 nm during the FRAP  
296 assay, which was carried out following a previously defined procedure <sup>19</sup>. An acetate buffer (pH  
297 3.6), 20 mM ferric chloride (FeCl<sub>3</sub>), and a FRAP solution diluted in 10 mM hydrochloric acid were  
298 combined in a volumetric ratio of 10:1:1 to create the working reagent. Before spectrophotometric  
299 examination, 0.1 mL of the diluted CSE was combined with 3.9 mL of the newly made working  
300 reagent, and the mixture was incubated for 20 minutes. The findings were presented as mg TAE/g,  
301 or µM Trolox equivalents per gram.

302 **2.11 Scanning Electron Microscopy (SEM) and X-ray Diffraction (XRD) of**  
303 **DCP**

304 The surface morphology of DCP following various extraction methods – including CE, MASE,  
305 EASE, and MEAE – was characterized using scanning electron microscopy (SEM). Prior to  
306 analysis, the extracted residues were dried at 85 °C for 24 hours in an oven until a constant weight  
307 was reached. The dried samples were mounted on carbon tape affixed to SEM sample stubs and  
308 examined using a gaseous secondary electron detector operating in SEM mode to assess changes  
309 in surface structure and morphological features <sup>16</sup>.

310 To evaluate the crystallinity of DCP, both untreated and treated samples were analyzed using  
311 X-ray diffraction (XRD). Measurements were performed with a D/max-RAX diffractometer (D8  
312 Advance, Bruker, Germany). The cellulose crystallinity index (CCI) was subsequently calculated  
313 using Equation (8), allowing for quantitative comparison of structural modifications resulting from  
314 the different extraction treatments <sup>20</sup>.

$$315 CCI = \frac{I_{cry} - I_{amp}}{I_{cry}} \times 100\% \quad (8)$$

316 The  $I_{cry}$  and  $I_{amp}$  are the intensity of the crystalline areas at 022.5 and the amorphous intensity  
317 at 018.

318 **2.12 Statistical analysis**

319 To ensure reproducibility, all experimental procedures were carried out in triplicate. The mean  
320 values and their accompanying standard deviations were used to express the results. OriginPro  
321 software (2022 version, OriginLab) was used to visualize data for individual variables, and Design  
322 Expert (version 13, Stat-Ease Inc., USA) was used to generate three-dimensional response surface  
323 graphs showing how experimental elements interacted. Minitab software (version 19.1) was used  
324 to perform statistical analyses, including analysis of variance (ANOVA), using a 95% confidence  
325 level ( $\alpha = 0.05$ ) for statistical significance.



326 **3 Results and Discussion**327 **3.1 Properties of Solvents**328 **3.1.1 FTIR**

329 The functional groups and hydrogen bonding interactions found in several NDES were  
330 examined using FTIR spectroscopy; the corresponding spectra are shown in Figure 1. Hydrogen  
331 bonds between the hydroxyl groups of polyols and carboxylic acids are indicated by a large O–H  
332 stretching vibration band seen between  $3060\text{ cm}^{-1}$  and  $3700\text{ cm}^{-1}$ <sup>21</sup>. Additionally, N–H stretching  
333 bands detected in the range of  $3447\text{--}3349\text{ cm}^{-1}$  suggest hydrogen bonding interactions between  
334 the tertiary ammonium groups of choline chloride and carboxylic acids. A characteristic peak  
335 around  $1709\text{--}1730\text{ cm}^{-1}$  was attributed to the C=O stretching vibrations of carboxylic acids such  
336 as lactic acid, citric acid, and acetic acid. Peaks near  $1645\text{ cm}^{-1}$  across all samples corresponded  
337 to C=C stretching vibrations<sup>22</sup>. Bands in the  $1195\text{--}1397\text{ cm}^{-1}$  range provided additional proof of  
338 hydrogen bonding between the C=O group of carboxylic acids and the tertiary ammonium group  
339 of choline chloride. Similar vibrations were detected in choline chloride-based systems at  $1480\text{ cm}^{-1}$   
340 and  $1415\text{ cm}^{-1}$ , whereas peaks at  $1458\text{ cm}^{-1}$  and  $1376\text{ cm}^{-1}$  were linked to  $-\text{CH}_3$  bending and  
341  $-\text{CH}$  bending vibrations, respectively, for lactic acid-based NDESs. The stretching and bending  
342 vibrations of the C–H, C–C, C–O, and OCO groups were associated with broader absorption bands  
343 in the  $1195\text{--}953\text{ cm}^{-1}$  area, suggesting structural complexity in the NDES matrices<sup>23</sup>. These  
344 spectral features align with previous studies on choline chloride-based NDESs, such as those  
345 involving *Castanea mollissima*<sup>24</sup>, thereby confirming the successful formation of NDESs through  
346 hydrogen bonding between carboxylic acids and both polyols and choline chloride



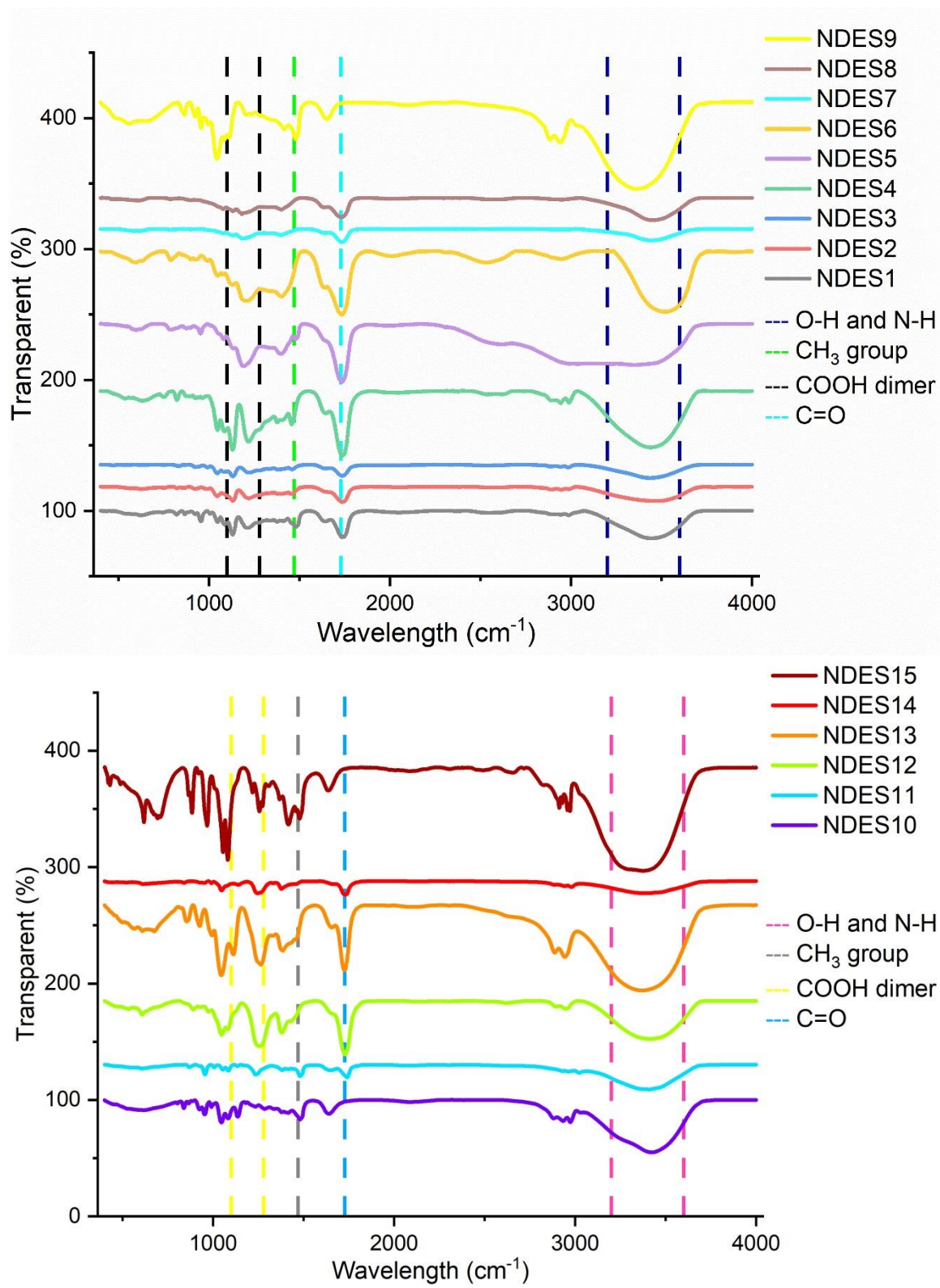


Figure 1. FTIR Spectra of NDES



349

### 3.1.2 Density

350 One of the primary physicochemical characteristics of NDES is its density, which directly  
351 impacts the effectiveness of extraction and separation procedures. As seen in Table 1, the densities  
352 of the various NDESs range greatly, ranging from 1.032 g/mL (Ace-Pro) to 1.444 g/mL (Ci-Pro),  
353 suggesting that their composition and intermolecular interactions are important factors. All tested  
354 NDESs exhibited densities greater than 1 g/mL, which is considerably higher than those of  
355 common organic solvents, such as ethanol and hexane.

356 The density of NDESs reflects the structural differences and the extent of interaction between  
357 their HBD and HBA components<sup>25</sup>. Density indicates the strength of the hydrogen bond network  
358 formed within the NDES, which in turn influences the solvent's stability and its ability to dissolve  
359 target compounds. Among the tested solvents, citric acid-based NDES (Ci-Pro) exhibited the  
360 highest density at 1.444 g/mL. This trend can be attributed to citric acid's multiple hydroxyl and  
361 carboxyl groups, which facilitate the development of a vast network of hydrogen bonds. In  
362 contrast, acetic acid-based NDES (Ace-Pro) showed the lowest density at 1.032 g/mL, likely due  
363 to its shorter carbon chain and fewer functional groups for hydrogen bonding. This trend aligns  
364 with previous findings that NDES formed with longer-chain or more hydroxylated organic acids  
365 tend to have higher densities. Additionally, NDES based on organic acids generally have higher  
366 densities than those based on polyols, as sugar-derived components, despite being denser in their  
367 pure form, tend to form less compact hydrogen-bonding networks in NDES mixtures<sup>26</sup>.

368

### 3.1.3 pH

369 The pH value of NDES solvents plays a critical role, influencing their chemical reactivity,  
370 solution stability, and biological safety. As shown in Table 1, the pH values of NDES range from  
371 -1.67 (Ci-Pro) to 3.36 (Gly-Cho), reflecting the varying acid–base characteristics of their  
372 constituent components. Since pH is the negative logarithm to the base 10 of H<sup>+</sup> concentration,  
373 values greater than 1 mol/L result in a negative pH. Among the NDESs formulated with organic  
374 acids as HBD, those based on citric acid (e.g., Ci-Pro, Ci-Ery) exhibit the lowest pH values. This  
375 trend aligns with the fact that citric acid has a low first pKa (~3.1), indicating a strong tendency to  
376 release protons (H<sup>+</sup>), thereby creating a more acidic medium<sup>27</sup>. Furthermore, the multiple carboxyl  
377 and hydroxyl groups on citric acid facilitate the formation of a dense hydrogen bonding network,  
378 which stabilizes the system and maintains a consistently low pH level. Although acetic acid has a  
379 higher pKa than lactic acid, the NDES prepared with acetic acid (e.g., Ace-Pro) display higher pH  
380 values than those made with citric acid. This can be attributed to the weaker hydrogen bonding  
381 interactions in acetic-based NDES, which result in a lower capacity to stabilize and retain free H<sup>+</sup>  
382 ions in the solution. Consequently, this leads to a relatively higher pH compared to citric-based  
383 systems.

384

### 3.1.4 Effect of NDES types

385 A total of fifteen NDESs were prepared by combining HBDs (lactic acid, citric acid, and acetic  
386 acid) with hydrogen bond acceptors HBAs (glycerol, choline chloride, erythritol, and 1,2-



387 propanediol). Notably, glycerol, erythritol, and 1,2-propanediol functioned dually as both HBA  
388 and HBD. The extraction performance of these NDESs was assessed under standardized  
389 conditions: a SLR of 1:20 g/mL, WC of 20% (w/w), MP of 728 W for 2 minutes, followed by  
390 enzymatic treatment with 30 U/g of EC and incubation at 50 °C for 90 minutes. Figure 2A presents  
391 the TPC and TFC extracted from *Coriandrum sativum* using the fifteen NDES formulations. The  
392 results revealed that the Gly-Cho (NDES9) exhibited the highest extraction performance, yielding  
393  $11.31 \pm 0.27$  mg GAE/g of total phenolics and  $16.92 \pm 1.10$  mg RE/g of total flavonoids.  
394 Conversely, Ci-Ery (NDES8) showed the lowest TPC recovery ( $3.23 \pm 1.05$  mg GAE/g), while  
395 Ci-Cho (NDES5) produced the lowest TFC yield ( $1.09 \pm 0.16$  mg RE/g).

396 The extraction efficiency of NDES is strongly influenced by solvent polarity, which determines  
397 the solubility and interaction between the solvent and target compounds. When the polarity of the  
398 solvent is compatible with that of the solute, it enhances solubility, promotes efficient mass  
399 transfer, and consequently results in higher extraction yields<sup>28</sup>. The partition coefficient (log P)  
400 serves as an indicator of molecular polarity, where smaller log P values reflect greater polarity of  
401 compounds or solvents. Among the HBDs, glycerol demonstrates a notably low log P of  $-1.76$ <sup>29</sup>,  
402 signifying its high polarity. Likewise, HBA choline chloride exhibits pronounced ionic and polar  
403 characteristics, allowing for strong interactions with hydrophilic solutes, such as phenolic  
404 compounds. Beyond polarity, the physicochemical characteristics of NDESs play a crucial role in  
405 determining their efficiency in recovering bioactive compounds. Excessive acidity in solvents can  
406 promote degradation or ionization of sensitive molecules, consequently lowering extraction  
407 efficiency<sup>30</sup>. In this study, NDES9 (pH = 3.36) provided an optimal medium for the stabilization  
408 and solubilization of phenolic compounds. In contrast, highly acidic solvents such as NDES8 (pH  
409 =  $-1.59$ ) and NDES5 (pH =  $-0.52$ ) may compromise the structural integrity of polyphenols,  
410 resulting in reduced recovery. Additionally, solvent density affects both phase dispersion and mass  
411 transfer behavior; higher densities, as observed in NDES8 (1.434 g/mL) and NDES5 (1.384 g/mL),  
412 can restrict solvent penetration into the plant matrix. With a moderate density of 1.164 g/mL,  
413 NDES9 achieved a better balance between diffusivity and interaction with the solid phase<sup>31</sup>.  
414 Therefore, NDES9 was chosen as the extraction medium for the recovery of phenolics and  
415 flavonoids in subsequent experiments.

416

417



418 

## 3.2 Single-factor experiments

419 

### 3.2.1 Impact of solid-to-liquid-ratio

420 The effects of the SLR on the extraction of TFC and TPC are illustrated in Figure 2B. The  
421 experiments were investigated using NDES9 with six different SLR levels: 1/10, 1/20, 1/30, 1/40,  
422 1/50, and 1/60 g/mL. As the SLR increased from 1/10 to 1/20 g/mL, the yields of both TPC and  
423 TFC rose significantly. In the study by Wong et al. (2013) on *Phyllanthus niruri*, increasing the  
424 solvent-to-solid ratio from 10:1 to 14:1 significantly improved phenolic extraction and antioxidant  
425 activity. This enhancement is based on a strong concentration gradient between the solid phase  
426 and the solvent, which increases mass transfer. Therefore, the driving force for diffusion increased,  
427 facilitating the release of phenolic compounds into the solvent and improving extraction efficiency  
428 <sup>32</sup>. Beyond the peak point, both TPC and TFC yields gradually declined. The observed decrease  
429 can be ascribed to an excessive amount of solvent, which lowers microwave energy absorption per  
430 unit mass of solid. This leads to a reduction in energy density, thereby weakening the thermal  
431 effects for extraction. As a result, the disruption of plant cellular structures to release bioactive  
432 compounds is limited <sup>33</sup>. Overall, the SLR of 1/20 g/mL was identified as the most favorable  
433 condition for maximizing the recovery of both TPC and TFC from coriander using the MEAE  
434 process.

435 

### 3.2.2 Impact of water content

436 The effects of WC in the NDES9 on the extraction of TFC and TPC are illustrated in Figure  
437 2C. In this experiment, water was added to the extraction solvent at 0%, 10%, 20%, 30%, 40%,  
438 and 50%. As WC increased from 0% to 20%, TPC and TFC content extraction increased  
439 significantly. Since water has a high dielectric constant and can efficiently absorb microwave  
440 energy, this improvement can be attributed to the better dielectric characteristics of the water-  
441 solvent mixture. Therefore, higher WC promotes matrix swelling and enhances the heating  
442 efficiency, releasing more phenolic and flavonoid compounds <sup>17</sup>. However, when the water content  
443 exceeded 20%, TPC and TFC yields declined. This trend aligns with research on *M. communis*  
444 leaves, which showed that TPC yield was lower at 20% ethanol (80% water) and peaked at 40%  
445 ethanol (60% water). This illustrates that excessive water content increases the solvent polarity but  
446 reduces the solubility of target compounds, according to the "like dissolves like" principle <sup>16</sup>. When  
447 the WC in NDES is excessive, the hydrogen bonds among NDES molecules are broken (Figure  
448 S1). This phenomenon reduces the interaction between NDES and phenolic compounds, thereby  
449 decreasing the effectiveness of the extraction process. Based on these observations, the effective  
450 water content for extracting TFC was 20%, while TPC showed the highest yield at 10% WC.



451                   **3.2.3 Impact of microwave power**

452                   The results of single-factor experiments for the extraction of phenolics and flavonoids from MP  
453                   are shown in Figure 2D. Experiments were tested using NDES9 with MP at 5 different levels: 280  
454                   W, 728 W, 1022 W, 1232 W, and 1400 W. When the MP increased from 280 W to 728 W, TPC  
455                   and TFC rose significantly. Excessively high power can rapidly increase the solution temperature,  
456                   leading to the degradation of heat-sensitive compounds, excessive solvent evaporation, and even  
457                   damage to the raw materials <sup>34</sup>. However, since then, both TPC and TFC values have remained  
458                   constant, then decreased significantly at higher power. The authors evaluated the effect of different  
459                   MP levels on the antioxidant activity of phenolic compounds from Roselle (*Hibiscus sabdariffa*  
460                   Linn). Due to the breakdown of heat-sensitive chemicals and a decrease in water content acting as  
461                   the solvent, the results demonstrated that the total anthocyanin and vitamin C content rose from  
462                   100 W and peaked at 325 W (13.8591 mg/100g) before declining at higher power levels <sup>35</sup>. Low  
463                   power is insufficient to break down plant cell walls, making it difficult for compounds to be  
464                   released. It also reduces cavitation effects and slows down diffusion. Therefore, 728 W is identified  
465                   as the optimal MP level, achieving the highest extraction efficiency for both TPC and TFC from  
466                   coriander.

467                   **3.2.4 Impact of microwave time**

468                   The results of single-factor experiments for phenolics and flavonoids extraction of MT are  
469                   shown in Figure 2E. Experiments were tested with microwave durations ranging from 30 seconds  
470                   to 4 minutes. For TPC, a relatively high value is observed at 30 seconds, before reaching its peak  
471                   at 3 minutes. Similarly, for TFC, the improvement in extraction efficiency is even more  
472                   pronounced. Starting at 30 seconds, TFC increases significantly at 1 minute and reaches its highest  
473                   value at 2 minutes. However, extending the microwave time to 3 minutes does not further enhance  
474                   the yield and may even cause a decline in TFC. By 4 minutes, both TPC and TFC show a more  
475                   evident reduction. In the experiment, the authors evaluated the effect of different microwave  
476                   durations on extracting Rhein and Emodin compounds from *Rheum palmatum* L. The results  
477                   showed that the extraction efficiency increased as the microwave time increased from 30 to 50  
478                   seconds. A duration of 50 seconds was selected, as more prolonged exposure (80 seconds) led to  
479                   partial degradation of Rhein and Emodin <sup>36</sup>. A short microwave time may not be sufficient to  
480                   disrupt the cell structure and release the target compounds. On the other hand, prolonged heat  
481                   exposure from excessive microwave radiation may cause the oxidation of phenolic compounds <sup>37</sup>.  
482                   Therefore, the time differs for each compound group: 3 minutes is the best condition for phenolic  
483                   recovery, while 2 minutes is the most efficient way to extract coriander's flavonoids.

484                   **3.2.5 Impact of enzyme concentration**

485                   The effect of EC on the extraction of phenolic and flavonoid compounds was evaluated, with  
486                   the results presented in Figure 2F. The MEAE process was investigated at enzyme concentrations  
487                   ranging from 10 to 50 U/g. An increase in EC from 10 to 30 U/g resulted in approximately a  
488                   twofold increase in TPC and a 1.3-fold increase in TFC. This enhancement is attributed to the



489 greater formation of enzyme-substrate complexes, which facilitated more effective hydrolysis of  
490 cell wall components, thereby enhancing the release of phenolic and flavonoid compounds.  
491 However, a further increase to 50 U/g led to a decline in extraction efficiency, with TPC and TFC  
492 yields decreasing by 1.24- and 1.20-fold, respectively. Excessive enzyme concentrations may  
493 accelerate the hydrolysis of bound bioactives into free forms, which, under elevated temperatures,  
494 become more mobile due to weakened hydrogen bonding within the solvent system. This increased  
495 mobility enhances their migration to the solvent interface, where exposure to oxidative and  
496 environmental stressors may promote degradation<sup>38</sup>. Similar findings were reported in studies  
497 involving *Acanthopanax senticosus*, where high enzyme concentrations adversely affected  
498 flavonoid recovery<sup>39</sup>. These results emphasize the importance of optimizing enzyme dosage to  
499 prevent compound degradation and ensure maximum extraction efficiency. Based on these  
500 observations, an enzyme concentration of 30 U/g was identified as optimal for efficiently  
501 extracting phenolics and flavonoids from DCP.

### 502 3.2.6 Impact of enzyme incubation time

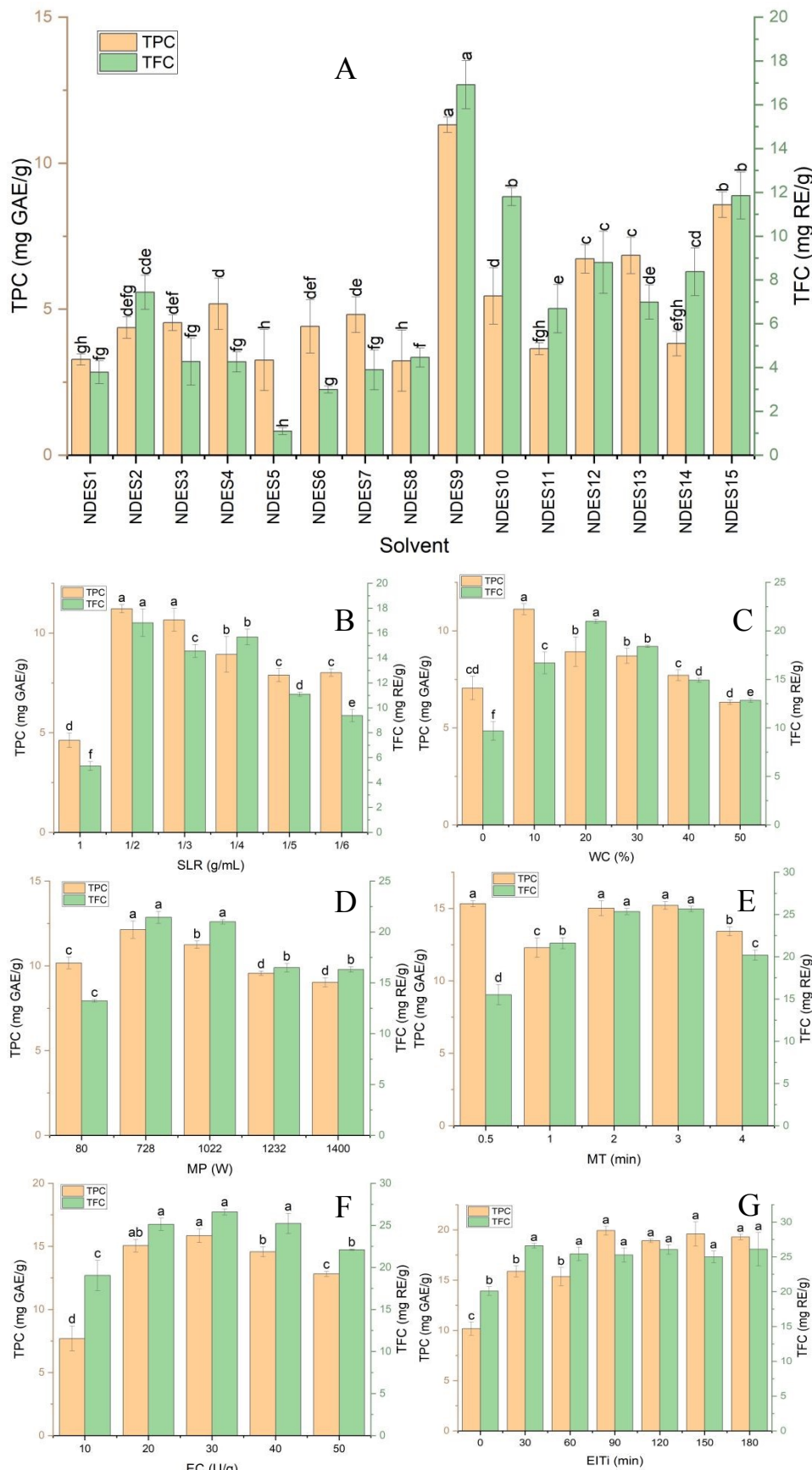
503 The effect of EIT on the extraction of phenolic and flavonoid compounds by NDES9 was  
504 evaluated, with the results presented in Figure 2G. Experiments were performed using varying  
505 incubation times (0 - 150 minutes). Without incubation (0 minutes), TPC and TFC exhibited the  
506 lowest yields, indicating limited extraction efficiency. This trend is likely due to the lack of  
507 interaction between the cellulase enzyme and the plant cell wall matrix, which prevents effective  
508 hydrolysis of cellulose chains and hinders the release of bound bioactive compounds. The rigid  
509 cellulose structure in DCP resists enzymatic breakdown, resulting in minimal release of  
510 compounds. Maximum extraction yields were achieved at 90 minutes for TPC (a 19.93% increase)  
511 and 30 minutes for TFC (a 26.60% increase), suggesting distinct extraction kinetics for phenolic  
512 and flavonoid compounds. The enzymatic degradation of cellulose enhances the porosity of the  
513 plant matrix by creating fissures and channels, thereby improving mass transfer and facilitating  
514 the release of target compounds<sup>38</sup>. However, prolonged incubation beyond these optimal times  
515 significantly reduced extraction efficiency by 18.93% for TPC and 26.51% for TFC. This decline  
516 is attributed to the degradation of thermolabile compounds under extended exposure to elevated  
517 temperatures, especially at the solvent interface, where oxidative and thermal stress can accelerate  
518 decomposition<sup>31</sup>. These findings are consistent with those reported by Vo et al. (2025), who  
519 observed a similar trend during the extraction of phenolics and flavonoids from *Elsholtzia ciliata*  
520<sup>31</sup>. In conclusion, an EIT of 90 minutes for TPC and 30 minutes for TFC was selected as suitable  
521 for extracting phenolics and flavonoids.

522 The difference in retention durations between TFC and TPC was determined based on  
523 preliminary experiments. These trials revealed that flavonoid extraction reached equilibrium faster  
524 than phenolic extraction under similar experimental conditions. Therefore, a shorter retention time  
525 was selected for TFC to prevent unnecessary exposure and potential thermal degradation, while a  
526 longer duration was maintained for TPC to ensure complete recovery of phenolic compounds.  
527 Based on the experimental results investigating the effects of microwave and enzyme treatment



528 duration, the appropriate time range was selected according to the recovery yields of phenolic and  
529 flavonoid compounds. The time point yielding the highest phenolic and flavonoid contents was  
530 designated as the center point, while the upper and lower boundaries were determined by the time  
531 points immediately preceding and following the center point, respectively. This approach enabled  
532 the selection of an optimal time range based on single-factor experiments. The investigation of  
533 time effects can also be considered a form of isothermal kinetic study.





535 **Figure 2.** MEAE conditions and their impact on TPC and TFC. NDESs' effect on TPC and TFC  
536 (A). SLR's (g/mL) effect on TPC and TFC (B). WC's (%) effect on TPC and TFC (C). MP's (W)  
537 effect on TPC and TFC (D). MT's (min) effect on TPC and TFC (E). EC's (U/g) effect on TPC and  
538 TFC (F). EIT's (min) effect on TPC and TFC (G). The letters a, b..., and h represent statistically  
539 significant differences

### 540 3.3 Factor evaluation and optimization

#### 541 3.3.1 Evaluating the significance of MEAE parameters

542 The Plackett-Burman Design (PBD) model was employed to identify the key factors influencing  
543 TPC and TFC extraction yields, as presented in Table S3 and Table S4. The coefficients exhibiting  
544 an absolute *t*-value greater than the critical threshold of 2.57 were deemed statistically significant,  
545 while those with  $|t\text{-value}| < 2.57$  were considered insignificant. These effects are quantitatively  
546 described by the regression equations presented in Equations (9) and (10). The model evaluated  
547 SLR (A), WC (B), MP (C), MT (D), EC (E), and EIT (F) –on phenolic and flavonoid recovery  
548 from DCP. Regarding the ANOVA results in Table S5, the model demonstrated strong predictive  
549 performance, with coefficients of determination ( $R^2$ ) of 97.11% and an adjusted coefficient of  
550 determination (Adj  $R^2$ ) of 90.94% for TPC. For TFC, the coefficients of determination ( $R^2$ ) of  
551 95.88% and the adjusted (Adj  $R^2$ ) of 93.63% indicate its adequacy for accurately modeling the  
552 experimental data. As illustrated in Figure 3A, EC ( $|t\text{-value}| = 6.73$ ), MP ( $|t\text{-value}| = 6.44$ ), and MT  
553 ( $|t\text{-value}| = 4.37$ ) were significant positive contributors to TPC recovery. According to earlier  
554 research, MP had a major impact on TPC recovery from *Euphorbia hirta* leaves<sup>40</sup>. Meanwhile,  
555 Figure 3B reveals that SLR ( $|t\text{-value}| = 11.99$ ), WC ( $|t\text{-value}| = 3.40$ ), and EIT ( $|t\text{-value}| = 2.68$ )  
556 significantly enhanced TFC extraction. Previous studies have indicated that WC plays a crucial  
557 role in modulating the efficiency of flavonoid extraction. In particular, investigations on *Perilla*  
558 leaves highlighted WC as a key determinant influencing (TFC) recovery, due to its effect on  
559 solvent polarity and dielectric behavior during MASE<sup>41</sup>. Based on these findings, EC, MP, and  
560 MT were selected for optimizing phenolic extraction, while SLR, WC, and EIT were identified as  
561 the critical variables influencing flavonoid yield.

$$562 y_{TPC} = 17.659 + 1.553 \cdot x_3 + 1.055 \cdot x_4 + 1.623 \cdot x_5 \quad (9)$$

$$563 y_{TFC} = 17.608 + 6.553 \cdot x_1 + 1.859 \cdot x_2 - 1.465 \cdot x_6 \quad (10)$$

564



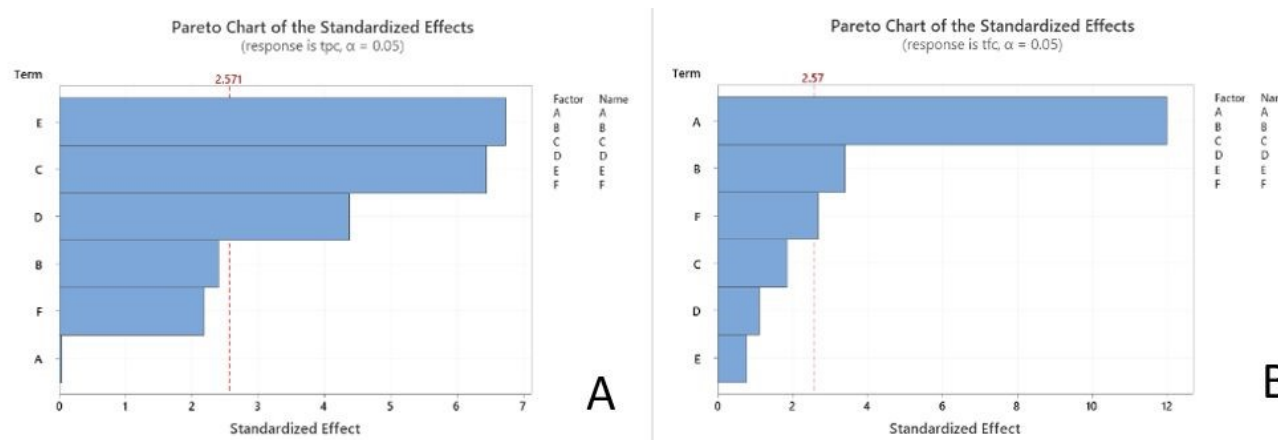


Figure 3. The Plackett-Burman Design's Pareto charts demonstrate how crucially extraction parameters affect the yield of the target compound. (A): How these parameters affect TPC yield; (B): How these parameters affect TFC yield. The variables analyzed included SRL (A), WC (B), MP (C), MT (D), EC (E), and EIT (F).

### 3.3.2 Optimization of the MEAE process

In this study, fourteen experimental runs (Table S6) were conducted to investigate the synergistic effects of EC, MP, and MT on the extraction efficiency of TPC from DCP, while all other variables were maintained at their central levels. Similarly, another set of fourteen experiments (Table S7) was conducted to evaluate the combined effects of SLR, WC, and EIT on the extraction yield of TFC. The Box-Behnken Design (BBD) was applied to analyze the individual and interactive effects of these process parameters on the performance of the MASE and EASE systems. Furthermore, three-dimensional response surface plots illustrated the interactive relationships between the independent variables and their corresponding responses. The regression models describing the correlations between the selected process variables and the responses – TPC and TFC – are presented in Equations (11) and (12), respectively:

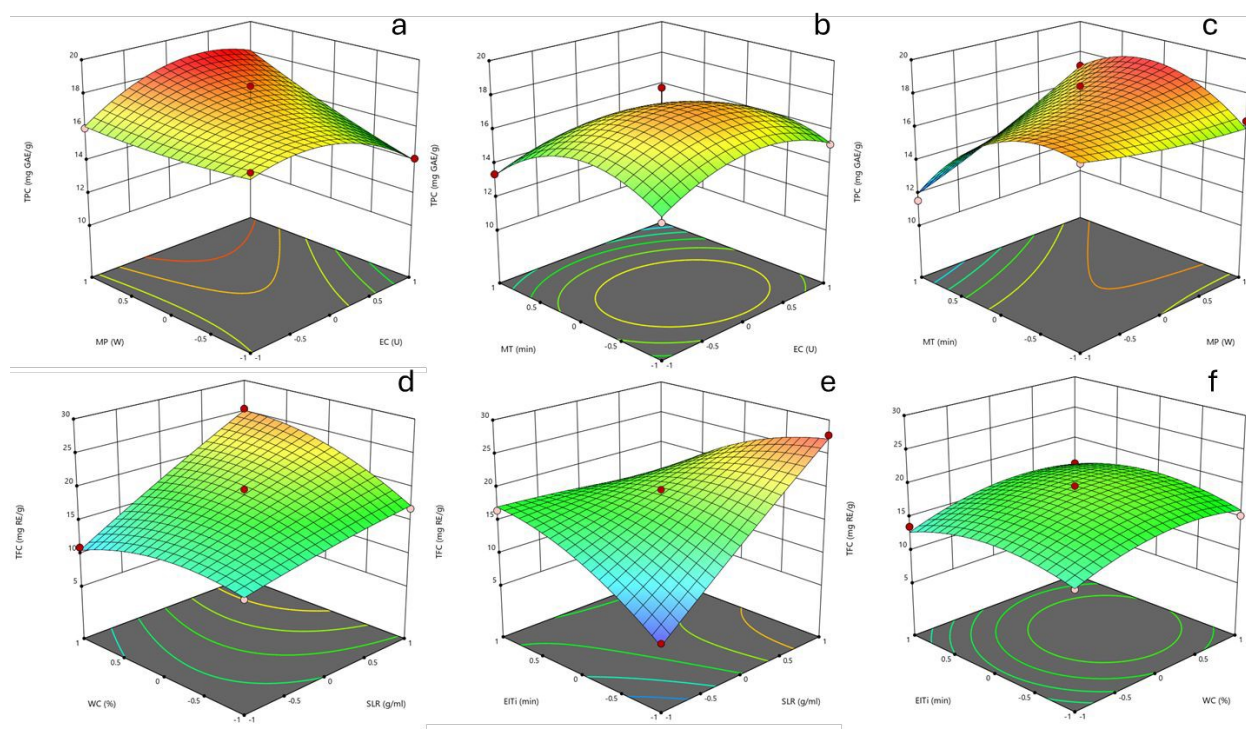
$$y_{TPC} = 17.39 + 0.9562 \cdot x_3 - 1.03 \cdot x_4 + 1.59 \cdot x_{34} - 2.04 \cdot x_4^2 - 1.45 \cdot x_5^2 \quad (11)$$

$$y_{TFC} = 18.95 + 4.69 \cdot x_1 + 1.30 \cdot x_2 + 2.62 \cdot x_{12} - 5.81 \cdot x_{16} - 2.05 \cdot x_2^2 - 2.23 \cdot x_6^2 \quad (12)$$

The data were subjected to analysis of variance (ANOVA), and the results, as summarized in Table S8, indicate statistically significant  $p$ -values ( $p < 0.05$ ) for both TPC and TFC, along with high adjusted  $R^2$  values of 0.8032 for TPC and 0.9644 for TFC. These findings validate the adequacy of the second-order regression models, demonstrating their strong agreement with the experimental data and reliable predictive capability. The variables EC, MP, and MT, as well as their interactions, had a considerable impact on the extraction efficiency of phenolics. In contrast, the TFC yield was predominantly affected by SLR, WC, EIT, and their interactions.



590 Based on Figure 4, the interactive effects of MEAE conditions on TPC and TFC are clearly  
 591 observed. TPC gradually increases with the simultaneous increase in MP and EC, reaching a peak  
 592 at higher levels of both factors. Notably, the combination of MT and MP significantly enhances  
 593 TPC, highlighting the crucial roles of thermal energy and extraction duration in releasing phenolic  
 594 compounds. For TFC, the interaction between WC and SLR indicates that both factors have a  
 595 positive influence on TFC, particularly with increased SLR. Furthermore, a substantial increase in  
 596 TFC is observed when both SLR and EIT are elevated, suggesting that extending enzymatic  
 597 treatment time in a more diluted solvent system effectively promotes flavonoid release.



598  
 599 **Figure 4.** 3D response surface visualizations exhibiting the interactive impacts of MEAE  
 600 conditions on TPC (a-c) and TFC (d-f)

601 **3.3.3 Model validation**

602 Validation experiments were conducted under the optimal conditions for MEAE to evaluate the  
 603 reliability of the developed regression models, as determined for each target compound. Using the  
 604 Box-Behnken Design (BBD), the optimal extraction parameters for maximizing TPC and TFC  
 605 from DCP were established. For TPC, the optimal conditions included a SLR of 1/20 g/mL, WC  
 606 of 10% (w/w), MP of 1022 W, MT of 2.6 minutes, EC of 40 U/g, EIT of 90 minutes, and EITem  
 607 of 50 °C. In contrast, the optimal conditions for TFC are as follows: SLR of 1/30 g/mL, WC:  
 608 23.7% (w/w), MP: 728 W, MT: 2 minutes, EC: 30 U/g, EIT: 30 minutes, and EITem: 50 °C. The  
 609 results of the validation experiments, presented in Table S9, revealed prediction error rates of



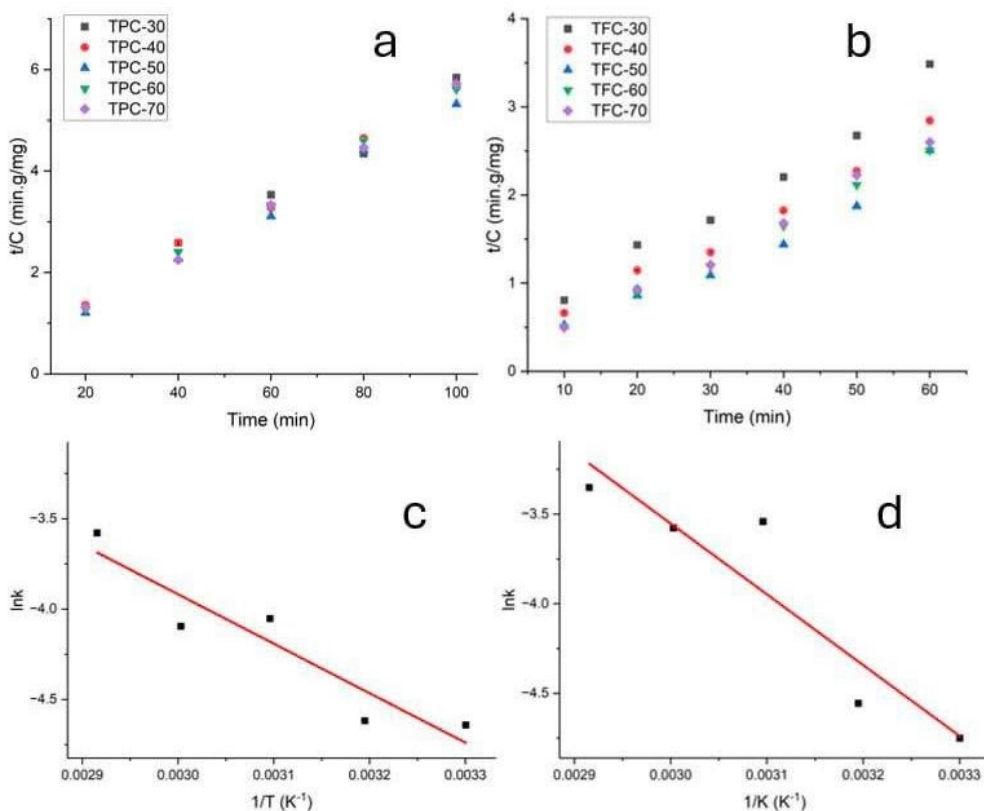
610 2.51% for TPC and 5.80% for TFC, confirming the robustness and predictive accuracy of the  
611 regression models within the tested experimental range.

### 612 3.4 Second-order extraction kinetic models

613 To scale these processes for industrial applications, the EASE and MASE extraction kinetic  
614 modeling of TFC and TFC is crucial. While keeping the other parameters at ideal levels, kinetic  
615 experiments were carried out for the MASE process at different temperatures (30, 40, 50, 60, and  
616 70 °C) and retention durations (20, 40, 60, 80, and 100 minutes for TPC and 10, 20, 30, 40, 50,  
617 and 60 minutes for TFC). The kinetic parameters, Arrhenius graphs, and second-order kinetic  
618 models of the phenolic and flavonoid extraction procedures are shown in Figure 5 and Table 6.  
619 The viability of second-order kinetic models for recovering flavonoids and phenolics using EASE  
620 and MASE processes under varied conditions was demonstrated by the high values of  
621 determination coefficients ( $R^2 \geq 0.9$ ). Due to the enhanced solvent diffusivity and solubility of  
622 bioactive compounds in the plant matrix, the  $h$  values rose as the temperature rose. Kenmogne  
623 Sidonie Béatrice et al. reported that the kinetics of the extraction process of total polyphenols from  
624 *Ximenia americana* roots using MASE showed that the pseudo-second-order kinetic model best  
625 described the process. The initial extraction rate ( $h$ ) increased significantly with temperature, with  
626 the rate at 80 °C being nearly six times higher than at 30 °C. The effective diffusion coefficient  
627 ( $D_{eff}$ ) also demonstrated a temperature dependence, ranging from  $2.215 \times 10^{-13}$  to  $7.232 \times 10^{-13}$  m<sup>2</sup>/s  
628 within the temperature range of 303K to 353K, and increasing with temperature. When analyzed  
629 using the Arrhenius model, the data yielded an activation energy ( $E_a$ ) of 14.436 kJ/mol with a high  
630 coefficient of determination ( $R^2 = 0.859$ ), confirming a strong relationship between temperature  
631 and mass transfer rate during the extraction process<sup>42</sup>.

632 Arrhenius graphs (1/T vs ln k) established from second-order kinetic models were used to  
633 evaluate the activation energy for extracting phenolics and flavonoids from DPC using MASE and  
634 EASE procedures. The activation energy represents the minimum energy required to overcome the  
635 chemical barrier and extract flavonoids and phenolics. Because of the increased activation energy,  
636 more energy is required to solubilize flavonoids and phenolics<sup>43</sup>. Furthermore, the mechanism for  
637 extraction activities is determined by the activation energy. Solubilization is the extraction method  
638 if  $E_a \geq 40$  kJ/mol. An activation energy of less than 20 kJ/mol indicates that diffusion is the  
639 dominant mechanism controlling the extraction. Diffusion and solubilization mechanisms are  
640 combined in the extraction process if  $E_a$  is between 20 and 40 kJ/mol<sup>42</sup>. TPC and TFC have been  
641 shown to have activation energy levels of 22.75 and 40.74 kJ/mol, respectively. While TFC is  
642 controlled by solubilization, TPC involves both diffusion and solubilization mechanisms. Given  
643 that flavonoids have a larger activation energy than phenolics, it is possible that flavonoid  
644 extraction will take place first, followed by phenolic extraction. Hobbi et al. used first-order and  
645 second-order kinetic models to study the extraction of polyphenols from apple pomace. Their  
646 findings indicated that the second-order model provided a better fit for predicting the influence of  
647 time and temperature on polyphenol recovery. Additionally, the study revealed that the extraction  
648 mechanism using 65% acetone, 50% ethanol, and water was primarily governed by diffusion<sup>44</sup>.



649  
650  
651  
652  
653

**Figure 5.** The variation of  $t/Ct$  in different periods during MEAE; (a): The variation of  $t/Ct$  in different times during MEAE – TPC; (b): The variation of  $t/Ct$  in different times during MEAE – TFC; The Arrhenius plot of the second-order kinetic models; (c): The Arrhenius plot of the second-order kinetic models of TPC; (d): The Arrhenius plot of the second-order kinetic models of TFC.

654

**Table 2.** Kinetic parameter of the extraction of phenolic and flavonoids from DCP

$T(^{\circ}\text{C})$	$C_s(\frac{mg}{g})$	$h(\frac{mg}{g.\text{min}})$	$k(\frac{g}{mg.\text{min}})$	$a(\frac{g}{mg})$	$b(\frac{g.\text{min}}{mg})$	$R^2_1$	$E_a(\frac{kJ}{mol})$	$\ln A_e$	$R^2_2$
TPC									
30	18.59	3.33	0.01	0.05	0.30	0.9902	22.75	0.05	0.8805
40	18.62	3.42	0.01	0.05	0.29	0.9928			
50	19.31	6.48	0.02	0.05	0.15	0.9965			
60	18.38	5.62	0.02	0.05	0.18	0.9981			
70	18.14	9.19	0.03	0.06	0.11	0.9972			
TFC									

30	19.88	3.42	0.01	0.05	0.29	0.9815	40.74	80097.51	0.8860	
40	23.70	4.56	0.01	0.04	0.21	0.9864				
50	26.25	19.96	0.03	0.04	0.05	0.9706				
60	24.63	18.38	0.03	0.04	0.05	0.9965				
70	23.53	27.03	0.05	0.04	0.03	0.9933				

655

656 

### 3.5 Antioxidant activity

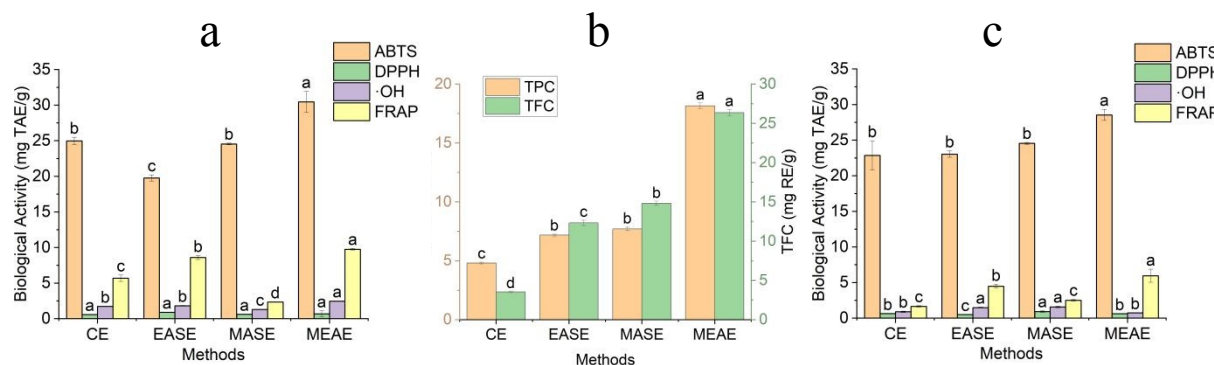
657 Figure 6 presents the results indicating statistically significant variations among the different  
 658 extraction methods regarding antioxidant activity and phytochemical content. Four extraction  
 659 approaches were evaluated, including microwave-assisted extraction (MASE), enzyme-assisted  
 660 extraction (EASE), conventional water extraction (CE), and a combined enzyme-microwave-  
 661 assisted extraction (MEAE). Among these, the MEAE technique demonstrated substantial  
 662 biological capacities for both TPC ( $18.15 \pm 0.25$  mg GAE/g) and TFC ( $26.36 \pm 0.41$  mg RE/g).  
 663 Four assays were used to assess the extracts' antioxidant capacity: DPPH, FRAP, ABTS, and  
 664 hydroxyl radical ( $\bullet\text{OH}$ ) scavenging. Due to the synergistic effect of the two extraction mechanisms,  
 665 including physical and biological, MEAE consistently yields considerable results in four  
 666 antioxidant assays (FRAP, ABTS,  $\bullet\text{OH}$ , and DPPH), as presented in Figure 6a and c. Under the  
 667 optimized extraction conditions for TPC, the MEAE method exhibited ABTS radical scavenging  
 668 capacity of  $30 \pm 1$  mg TAE/g, FRAP activity of  $9.8 \pm 0.1$  mg TAE/g, DPPH radical inhibition of  
 669  $0.7 \pm 0.4$  mg TAE/g, and hydroxyl radical scavenging activity of  $2.46 \pm 0.05$  mg TAE/g. Similarly,  
 670 under the optimized TFC extraction conditions, MEAE achieved ABTS at  $28.5 \pm 0.8$  mg TAE/g,  
 671 FRAP at  $6.0 \pm 0.9$  mg TAE/g, DPPH at  $0.61 \pm 0.01$  mg TAE/g, and hydroxyl radical scavenging  
 672 activity at  $0.74 \pm 0.02$  mg TAE/g. This improvement is attributed to the combined action of  
 673 enzymatic hydrolysis, which degrades phenolic-carbohydrate-flavonoid complexes, and  
 674 microwave treatment, which promotes cell wall rupture and accelerates mass transfer. As a result  
 675 of this process, phenolic and flavonoid chemicals are released in their free forms, which typically  
 676 have more antioxidant activity than their bound counterparts. A similar study demonstrated that  
 677 enzyme-assisted extraction from Vietnamese balm yields higher recovery of bioactive compounds,  
 678 with superior DPPH, ABTS, and FRAP antioxidant activities compared to non-assisted extraction.

679 <sup>31</sup>. As a result, the order of antioxidant effectiveness among the extraction methods was MEAE >  
 680 MASE > EASE > CE. The authors evaluated the MASE process combined with EASE for  
 681 extracting compounds from *Punica granatum* peel and assessed their antioxidant activity. The  
 682 study demonstrated that combining EASE and MASE resulted in a superior synergistic effect in  
 683 recovering phenolic compounds from pomegranate peel, achieving maximum antioxidant activity.

684 The phenolic content obtained using the combined method reached 305 mg GAE/g, which was  
685 significantly higher than that obtained using individual methods: Conventional Solvent Extraction  
686 yielded only 94.6 mg GAE/g, EASE yielded 165.46 mg GAE/g, and MASE yielded 197.6 mg  
687 GAE/g<sup>45</sup>. Overall, the results highlight the efficiency of the combined microwave and enzyme-  
688 assisted extraction in enhancing the recovery of phenolic and flavonoid compounds, which possess  
689 potent antioxidant properties.

690 Given the established bioactivities of phenolic and flavonoid compounds, this research  
691 underscores their potential for large-scale extraction and industrial use. These compounds are  
692 commonly employed in processed foods to prevent lipid and protein oxidation, thereby extending  
693 shelf life and ensuring product stability. Beyond their antioxidant effects, they also exhibit notable  
694 antimicrobial properties, helping to control spoilage and pathogenic microorganisms. In broilers,  
695 dietary supplementation with polyphenols extracted from olive oil processing by-products  
696 enhanced meat antioxidant capacity<sup>46</sup>. The inclusion of gallic and linoleic acids improved lipid  
697 metabolism, productivity, and meat quality, as well as its antioxidant and antimicrobial properties<sup>46</sup>.  
698 Supplementation with oregano and laurel oils promoted growth performance and reduced lipid  
699 oxidation<sup>47</sup>, while rosemary extract in turkey diets effectively inhibited lipid oxidation and  
700 delayed meat spoilage<sup>46</sup>. Various snacks and beverages enriched with phenolics have recently  
701 been introduced, enhancing both sensory attributes and nutritional value. Additionally, extracts  
702 from *Coriandrum sativum* show great promise for use in dietary supplements, positioning them as  
703 a viable option for both the food and health sectors<sup>48</sup>. For example, coriander polyphenols have  
704 been reported to mitigate obesity and metabolic syndrome. Administration of coriander seeds to  
705 rats fed a high-cholesterol and high-triglyceride diet resulted in a hypolipidemic effect,  
706 accompanied by enhanced hepatic conversion of cholesterol to bile acids and increased fecal  
707 excretion<sup>49</sup>. In broiler chicks, dietary inclusion of whole coriander seeds significantly improved  
708 growth performance, body weight, feed intake, and feed conversion ratio<sup>46</sup>. In a human study  
709 conducted by Mexican researchers, volunteers received *C. sativum* seed powder, chia (*Salvia*  
710 *hispanica*) powder, or both for two months. Coriander supplementation increased antioxidant  
711 capacity and reduced glucose and cholesterol levels, while chia supplementation lowered  
712 cholesterol and triglycerides. The combined treatment further decreased glucose, cholesterol, and  
713 triglyceride levels, and all participants experienced weight loss<sup>50</sup>.





714  
 715 **Figure 6.** Antioxidant activity and phytochemical content of extracts under optimal conditions.  
 716 (a): Antioxidant activities of extracts from TPC optimized extraction conditions. (b): Phenolics  
 717 and Flavonoids content in extracts from TPC and TFC optimized extractions. (c): Summarizes the  
 718 comparative antioxidant capacities (FRAP, DPPH, ABTS, and  $\cdot\text{OH}$ ) of under-optimized TFC  
 719 conditions. The letters a, b, c, and d represent statistically significant differences

### 720 3.6 Surface Morphology and Crystalline Structure

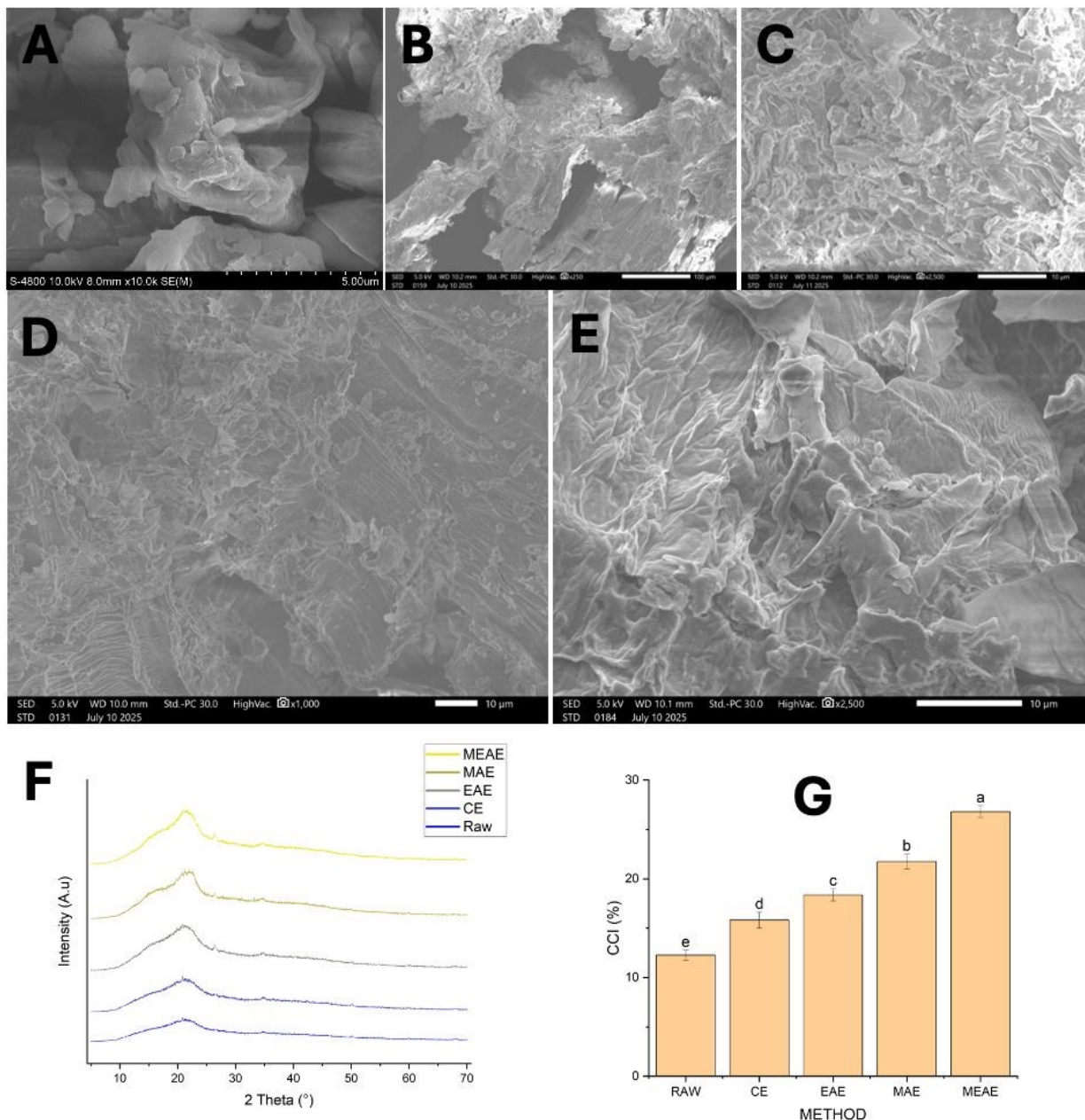
721 SEM was used to provide the surface morphological changes of the DCP before and after treatment.  
 722 Figure 7A-E illustrates the DCP's surfaces under different extraction conditions, revealing significant  
 723 structural alterations depending on the technique used. The CE sample (Figure 7B) shows a relatively  
 724 intact, dense surface structure with minimal cell wall disruption. The tightly bound cellular matrices  
 725 indicate limited cell rupture, which likely restricts the release of bioactive compounds, resulting in  
 726 lower extraction efficiency. The EASE sample (Figure 7C) exhibits disruption of the cellular structure.  
 727 The surface appears uneven with small cracks, likely caused by the enzymatic hydrolysis of cell wall  
 728 polysaccharides. This increases permeability and facilitates the release of phenolic compounds<sup>51</sup>. The  
 729 MASE sample (Figure 7D) reveals severe fragmentation and deep fissures across the surface,  
 730 characterized by layered and broken structures. These morphological changes are attributed to  
 731 localized microwave heating, which generates internal pressure and causes extensive cell rupture,  
 732 thereby enhancing the extraction of intracellular components<sup>52</sup>. The MEAE sample (Figure 7E)  
 733 displays the most pronounced surface disruption, with prominent exfoliation and sponge-like cavities.  
 734 The synergistic action of microwave and enzymatic treatment results in both cell wall weakening and  
 735 thermal-induced rupture.

736 X-ray diffraction (XRD) is a powerful analytical technique widely used to assess changes in the  
 737 crystalline structure of materials. It allows for the identification of crystalline phases and provides  
 738 detailed structural information without compromising sample integrity. In this study, XRD was  
 739 employed to evaluate the alterations in crystallinity of DCP subjected to various extraction methods,  
 740 including CE, EASE, MASE, and MEAE. The analysis primarily focused on determining the



741 Crystallinity Index (CCI), a parameter indicative of structural reorganization influenced by the applied  
742 treatments. Diffractograms were collected over a  $\theta$  range of  $5.00^\circ$  to  $70.01^\circ$ , with prominent peaks  
743 observed at approximately  $18^\circ$  and  $22.5^\circ$ , corresponding to the amorphous and crystalline regions,  
744 respectively (Figure 7F). The untreated DCP exhibited a CCI of  $12.27\% \pm 0.50\%$ , while samples  
745 treated with CE, EASE, MASE, and MEAE displayed progressively higher CCI values of  $15.81\% \pm$   
746  $0.80\%$ ,  $18.37\% \pm 0.60\%$ ,  $21.76\% \pm 0.75\%$ , and  $26.81\% \pm 0.60\%$ , respectively (Figure 7G). These  
747 results suggest that the combined MEAE process, integrating both microwave energy and enzymatic  
748 hydrolysis, induces the most substantial enhancement in crystallinity, likely due to its ability to  
749 effectively disrupt amorphous cell wall components and promote the realignment of crystalline  
750 domains. An increase in crystallinity was observed after the various extraction treatments, indicating  
751 that removing amorphous components such as lignin and hemicellulose led to greater exposure of  
752 crystalline cellulose, thereby increasing the Crystallinity Index (CCI)<sup>53</sup>. During the EASE process,  
753 NDES facilitated the partial solubilization of amorphous structures through selective interactions while  
754 preserving the crystalline regions. In contrast, MASE raised the temperature of the solvent system,  
755 enhancing the solubility of both amorphous cellulose and hemicellulose. The combined MEAE process  
756 amplified these effects synergistically, resulting in more effective disruption of amorphous domains  
757 and substantial enrichment of crystalline cellulose<sup>54</sup>. Consequently, the MEAE-treated samples  
758 exhibited the highest CCI, confirming its superior capability in enhancing the material's crystalline  
759 structure.





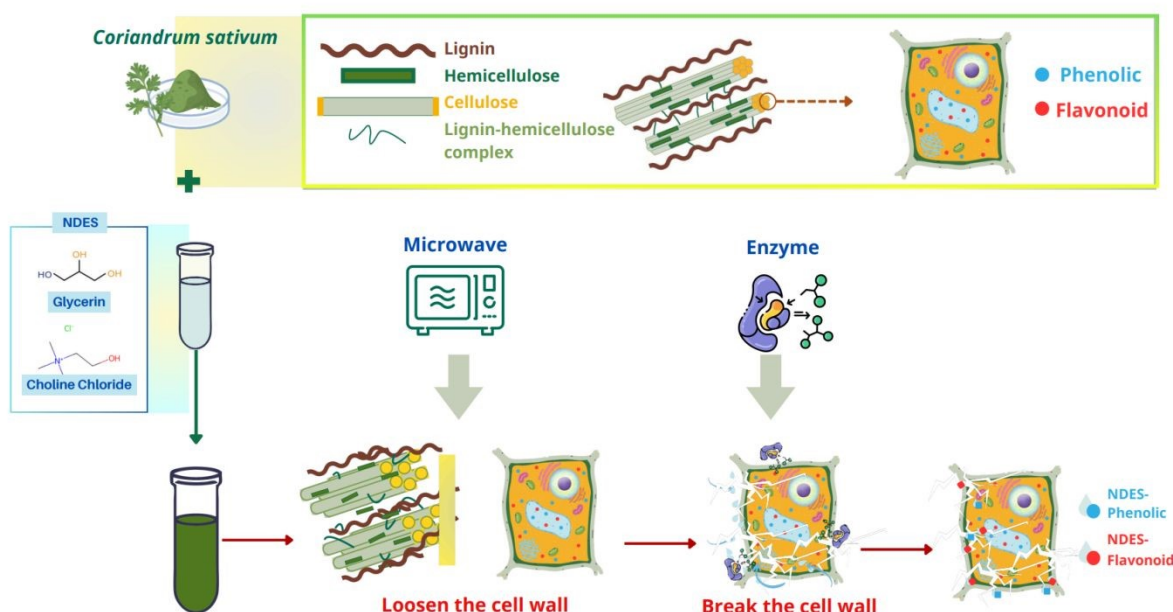
760

761 **Figure 7.** Surface morphology and Crystalline structure of DCP under different treatment  
 762 conditions. (A): Surface morphology of untreated DCP; (B): Surface morphology of DCP treated  
 763 with CE; (C): Surface morphology of DCP treated with NDES-based EASE; (D): Surface  
 764 morphology of DCP treated with NDES-based MASE; (E): Surface morphology of DCP treated  
 765 with NDES-based MEAE; Crystalline structure analysis (F) and CCI profiles (G) of untreated and  
 766 different treated NDES-based DCP. The letters a, b, c, d, and e represent statistically significant  
 767 differences



768 **3.7 The mechanism of natural deep eutectic solvents-based microwave-  
769 enzymatic-assisted extraction**

770 A comprehensive extraction mechanism underlying the MEAE technique can be inferred from  
771 the kinetic data, SEM observations, and XRD analysis (Figure 8). The microwave treatment  
772 induced localized heating and internal pressure, resulting in cell wall rupture and enhanced solvent  
773 penetration into plant tissues<sup>55</sup>. Concurrently, the enzymatic hydrolysis of polysaccharides  
774 weakened the cell wall matrix by breaking down cellulose and hemicellulose, facilitating mass  
775 transfer and compound release<sup>56</sup>. The NDES further contributed to this process by forming  
776 hydrogen bonds with cell wall components, partially dissolving amorphous lignin, and improving  
777 the solubility of phenolic and flavonoid compounds<sup>57</sup>. These synergistic effects collectively  
778 disrupted the plant structure, increased porosity, and exposed the crystalline cellulose regions  
779 observed in XRD patterns, resulting in a higher crystallinity index. The MEAE process effectively  
780 integrates physical and biochemical mechanisms, achieving efficient extraction while maintaining  
781 the structural stability of target bioactive compounds.



782  
783 **Figure 8.** The mechanism of the natural deep eutectic solvents-based microwave-enzymatic-  
784 assisted extraction process in recovering phenolics and flavonoids from *Coriandrum sativum*  
785 leaves.

786 **3.8 Reusability of solvent and Cost and energy estimation**

787 The reusability of the NDES was evaluated through five consecutive extraction cycles (Figure  
788 S2). For TPC, the first reuse retained  $94.36 \pm 2.90\%$  of the initial extraction yield, which gradually

declined to  $85.65 \pm 0.72\%$ ,  $76.25 \pm 0.97\%$ ,  $74.29 \pm 0.85\%$ , and  $68.90 \pm 1.45\%$  after the second to fifth cycles, respectively. Although a steady decrease was observed, more than 70 % of the extraction efficiency was maintained after five cycles, demonstrating satisfactory solvent durability. A similar trend was observed for TFC, with retention rates of  $91.67 \pm 1.81\%$ ,  $83.33 \pm 1.62\%$ ,  $82.63 \pm 5.18\%$ ,  $79.06 \pm 0.71\%$ , and  $78.66 \pm 0.52\%$  for the first through fifth reuses, respectively. Statistical analysis (one-way ANOVA,  $p < 0.05$ ) indicated that the differences between the first three cycles were insignificant, while significant decreases occurred from the fourth cycle onward. The gradual reduction in recovery efficiency may result from partial accumulation of residual plant pigments and polysaccharides in the solvent matrix, which can hinder mass transfer and reduce solvation efficiency. Nevertheless, TPC and TFC retained over 75-80 % of their initial extraction efficiency after five reuse cycles without additional purification, confirming the solvent's strong structural stability. Thus, the NDES9-based MEAE process shows the alignment with the principles of green chemistry, which can reduce the negative environmental impact of extraction process.

The total cost and energy requirements for the optimized MEAE process were calculated for a 1 L batch, taking into account both material and energy consumption (Table S10). The estimated material cost for recovering phenolic and flavonoid compounds from 1 kg of DCP using NDES9 was 10.53 \$USD/kg, whereas recovery using water required 7.6 \$USD/kg. The estimated energy cost for recovering phenolic and flavonoid compounds from 1 kg DCP using NDES9 was 8.2 \$USD, whereas recovery using water required 9.3 \$USD. Although operating cost for NDES9 extraction is higher than water extraction, the extraction efficiency of NDES9 is higher than water. Overall, the efficiency of operating cost using NDES9 is better than using water. Therefore, the NDES-based MEAE system has a high potential for large-scale extraction of phenolic and flavonoid compounds from plants.

#### 4 Conclusions

This study demonstrates that optimized MEAE conditions, based on statistical modeling, effectively enhance the recovery of antioxidants from *Coriandrum sativum* leaves. Among all tested NDESs, the glycerol-choline chloride system exhibited the highest extraction efficiency for both phenolic and flavonoid compounds. FTIR analysis confirmed the formation of hydrogen bonds between hydroxyl and carboxyl groups, verifying the solvent's structural stability and strong solvation ability. The optimal extraction conditions for TPC and TFC were generally similar, differing only in microwave extraction time and enzyme incubation time. The MT and EIT for TPC recovery are 2.6 and 90 minutes, whilst that of TFC recovery are 2 and 30 minutes. Kinetic modeling revealed that TPC extraction followed a combined diffusion-solubilization mechanism, whereas TFC extraction was primarily governed by solubilization. Improved extraction efficiency



824 resulted from the synergy of microwave-assisted cell disruption and enzyme-catalyzed hydrolysis,  
825 as supported by SEM and XRD evidence of cell wall rupture and increased crystallinity.  
826 Additionally, the NDES system demonstrated high reusability, maintaining an extraction  
827 efficiency of approximately 75% after several cycles, highlighting its potential as a green, efficient,  
828 and sustainable solvent for industrial-scale applications. The findings highlight the potential of the  
829 extract as a natural preservative to replace synthetic additives that may pose health risks. Moreover,  
830 the extract can be further processed into concentrated paste, capsules, or dried powder for  
831 incorporation into various food products such as beverages and snack foods. It also shows promise  
832 as a partial fat replacer in processed foods like fish balls and sausages, contributing to extended  
833 shelf life and improved product quality.

834

## 835 Abbreviations

836 DCP: Dried Coriander Powder; CE: Convectional Extraction; MASE: Microwave-Assisted  
837 Extraction; EASE: Enzyme-Assisted Extraction; MEAE: Microwave-Enzymatic-Assisted  
838 Extraction; TPC: Total Phenolic Content; TFC: Total Flavonoid Content; NDES: natural deep  
839 eutectic solvents; SLR: Solid-to-Liquid Ratio; WC: Water content; MP: Microwave Power; MT:  
840 Microwave Time; EC: Enzyme concentration; EIT: Enzyme Incubation Time; EITem: Enzyme  
841 Incubation Temperature; CSE: crude sample extract; ABTS: [2,2'-azino-bis(3-  
842 ethylbenzothiazoline-6-sulfonic acid)]; DPPH: (2,2-diphenyl-1-picrylhydrazyl); FRAP: (Ferric  
843 Reducing Antioxidant Power); SEM: scanning electron microscopy; XRD: X-ray diffraction; CCI:  
844 cellulose crystallinity index.

## 845 Funding Declaration

846 There are no funding sources for the manuscript.

## 847 Credit authorship contribution statement

848 Tan Phat Vo: Conceptualization, Methodology, Software, Formal analysis, Investigation, Data  
849 curation, Writing- original draft, Writing-review & editing, Visualization. Minh Thu Nguyen:  
850 Investigation, Formal analysis. Thuy Anh Nguyen: Writing - original draft, Visualization. Gia  
851 Vinh Nguyen: Investigation, Formal analysis. Hoang Nhan Nguyen: Writing- original draft. Gia  
852 Bao Pham: Writing- original draft. Minh Hoa Ha: Investigation, Formal analysis. Dinh Quan  
853 Nguyen: Writing- original draft, Investigation, Formal analysis, Supervision.

## 854 Declaration of competing interest

855 The authors declare that they have no known competing financial interests or personal  
856 relationships that could have appeared to influence the work reported in this paper.



857 **Data availability**

858 Data will be made available on request.

859 **Acknowledgments**860 We acknowledge Ho Chi Minh City University of Technology (HCMUT), VNU-HCM for  
861 supporting this study.862 **References**

863 (1) Laribi, B.; Kouki, K.; M'Hamdi, M.; Bettaieb, T. Coriander (*Coriandrum sativum L.*) and its  
864 bioactive constituents. *Fitoterapia* **2015**, *103*, 9-26. DOI:  
865 <https://doi.org/10.1016/j.fitote.2015.03.012>.

866 (2) Wangensteen, H.; Samuelsen, A. B.; Malterud, K. E. Antioxidant activity in extracts from  
867 coriander. *Food Chemistry* **2004**, *88* (2), 293-297. DOI:  
868 <https://doi.org/10.1016/j.foodchem.2004.01.047>.

869 (3) Iqbal, I.; Wilairatana, P.; Saqib, F.; Nasir, B.; Wahid, M.; Latif, M. F.; Iqbal, A.; Naz, R.;  
870 Mubarak, M. S. Plant Polyphenols and Their Potential Benefits on Cardiovascular Health: A  
871 Review. *Molecules* **2023**, *28* (17). DOI: <https://doi.org/10.3390/molecules28176403>.

872 (4) Hansen, B. B.; Spittle, S.; Chen, B.; Poe, D.; Zhang, Y.; Klein, J. M.; Horton, A.; Adhikari, L.;  
873 Zelovich, T.; Doherty, B. W.; et al. Deep Eutectic Solvents: A Review of Fundamentals and  
874 Applications. *Chemical Reviews* **2021**, *121* (3), 1232-1285. DOI:  
875 <https://doi.org/10.1021/acs.chemrev.0c00385>.

876 (5) Alara, O. R.; Abdurahman, N. H.; Ukaegbu, C. I. Extraction of phenolic compounds: A review.  
877 *Current Research in Food Science* **2021**, *4*, 200-214. DOI:  
878 <https://doi.org/10.1016/j.crfs.2021.03.011>.

879 (6) Chan, C.-H.; Yusoff, R.; Ngoh, G.; Kung, F. *Extraction of Anti-diabetic Active Ingredient,  
880 Quercetin from Herbal Plant Using Microwave-assisted Extraction (MAE) Technique*; 2011. DOI:  
881 <https://doi.org/10.13140/2.1.3487.4885>.

882 (7) Chaliha, M.; David, W.; Edwards, D.; Pun, S.; Smyth, H.; Sultanbawa, Y. Bioactive rich  
883 extracts from *Terminalia ferdinandiana* by enzyme-assisted extraction: A simple food safe  
884 extraction method. *Journal of Medicinal Plants Research* **2017**, *11*, 96-106. DOI:  
885 <https://doi.org/10.5897/JMPR2016.6285>.

886 (8) Vo, T. P.; Nguyen, T. H. P.; Nguyen, V. K.; Dang, T. C. T.; Nguyen, L. G. K.; Chung, T. Q.;  
887 Vo, T. T. H.; Nguyen, D. Q. Extracting bioactive compounds and proteins from *Bacopa monnieri*  
888 using natural deep eutectic solvents. *PLOS ONE* **2024**, *19* (3), e0300969. DOI:  
889 <https://doi.org/10.1371/journal.pone.0300969>.

890 (9) Sakurai, Y. C.; Pires, I. V.; Ferreira, N. R.; Moreira, S. G.; Silva, L. H.; Rodrigues, A. M.  
891 Preparation and Characterization of Natural Deep Eutectic Solvents (NADESs): Application in the  
892 Extraction of Phenolic Compounds from Araza Pulp (*Eugenia stipitata*). *Foods* **2024**, *13* (13).  
893 DOI: <https://doi.org/10.3390/foods13131983>.

894 (10) Wu, L.; Li, L.; Chen, S.; Wang, L.; Lin, X. Deep eutectic solvent-based ultrasonic-assisted  
895 extraction of phenolic compounds from *Moringa oleifera* L. leaves: Optimization, comparison and



896 antioxidant activity. *Separation and Purification Technology* **2020**, *247*, 117014. DOI:  
897 <https://doi.org/10.1016/j.seppur.2020.117014>.

898 (11) Shraim, A. M.; Ahmed, T. A.; Rahman, M. M.; Hijji, Y. M. Determination of total flavonoid  
899 content by aluminum chloride assay: A critical evaluation. *LWT* **2021**, *150*, 111932. DOI:  
900 <https://doi.org/10.1016/j.lwt.2021.111932>.

901 (12) Pereira, L. M. S.; Milan, T. M.; Tapia-Blácido, D. R. Using Response Surface Methodology  
902 (RSM) to optimize 2G bioethanol production: A review. *Biomass and Bioenergy* **2021**, *151*,  
903 106166. DOI: <https://doi.org/10.1016/j.biombioe.2021.106166>.

904 (13) Ho, Y. S.; McKay, G. Pseudo-second order model for sorption processes. *Process  
905 Biochemistry* **1999**, *34* (5), 451-465. DOI: [https://doi.org/10.1016/S0032-9592\(98\)00112-5](https://doi.org/10.1016/S0032-9592(98)00112-5).

906 (14) Ran, H.; Zhang, X.; Long, J.; Wang, Z.; Zhuang, S.; Zhang, X.; Jiang, Y.; Zhang, J.; Wang,  
907 G. Ultrasound-assisted extraction of naringin from *Exocarpium Citri Grandis* using a novel ternary  
908 natural deep eutectic solvent based on glycerol: Process optimization using ANN-GA, extraction  
909 mechanism and biological activity. *Ultrasonics Sonochemistry* **2025**, *121*, 107551. DOI:  
910 <https://doi.org/10.1016/j.ultsonch.2025.107551>.

911 (15) Zhang, X.; Su, J.; Chu, X.; Wang, X. A Green Method of Extracting and Recovering  
912 Flavonoids from *Acanthopanax senticosus* Using Deep Eutectic Solvents. *Molecules* **2022**, *27* (3).  
913 DOI: <https://doi.org/10.3390/molecules27030923>.

914 (16) Dahmoune, F.; Nayak, B.; Moussi, K.; Remini, H.; Madani, K. Optimization of microwave-  
915 assisted extraction of polyphenols from *Myrtus communis* L. leaves. *Food Chemistry* **2015**, *166*,  
916 585-595. DOI: <https://doi.org/10.1016/j.foodchem.2014.06.066>.

917 (17) Rodsamran, P.; Sothornvit, R. Extraction of phenolic compounds from lime peel waste using  
918 ultrasonic-assisted and microwave-assisted extractions. *Food Bioscience* **2019**, *28*, 66-73. DOI:  
919 <https://doi.org/10.1016/j.fbio.2019.01.017>.

920 (18) Mukhopadhyay, D.; Dasgupta, P.; Sinha Roy, D.; Palchoudhuri, S.; Chatterjee, I.; Ali, S.;  
921 Ghosh Dastidar, S. A Sensitive In vitro Spectrophotometric Hydrogen Peroxide Scavenging Assay  
922 using 1,10-Phenanthroline. *Free Radicals and Antioxidants* **2015**, *6* (1), 124-132. DOI:  
923 <https://doi.org/10.5530/fra.2016.1.15>.

924 (19) Vu, H. T.; Scarlett, C. J.; Vuong, Q. V. Maximising recovery of phenolic compounds and  
925 antioxidant properties from banana peel using microwave assisted extraction and water. *Journal  
926 of Food Science and Technology* **2019**, *56* (3), 1360-1370. DOI: <https://doi.org/10.1007/s13197-019-03610-2>.

928 (20) Agarwal, U. P.; Ralph, S. A.; Baez, C.; Reiner, R. S.; Verrill, S. P. Effect of sample moisture  
929 content on XRD-estimated cellulose crystallinity index and crystallite size. *Cellulose* **2017**, *24* (5),  
930 1971-1984. DOI: <https://doi.org/10.1007/s10570-017-1259-0>.

931 (21) Pires, I. V.; Sakurai, Y. C.; Ferreira, N. R.; Moreira, S. G.; da Cruz Rodrigues, A. M.; da  
932 Silva, L. H. Elaboration and Characterization of Natural Deep Eutectic Solvents (NADESs):  
933 Application in the Extraction of Phenolic Compounds from pitaya. *Molecules* **2022**, *27* (23). DOI:  
934 <https://doi.org/10.3390/molecules27238310>.

935 (22) Zannou, O.; Koca, I. Greener extraction of anthocyanins and antioxidant activity from  
936 blackberry (*Rubus* spp) using natural deep eutectic solvents. *LWT* **2022**, *158*, 113184. DOI:  
937 <https://doi.org/10.1016/j.lwt.2022.113184>.



938 (23) Subashini, K.; Periandy, S. Spectroscopic (FT-IR, FT-Raman, UV, NMR, NLO) investigation  
939 and molecular docking study of 1-(4-Methylbenzyl) piperazine. *Journal of Molecular Structure*  
940 **2017**, *1134*, 157-170. DOI: <https://doi.org/10.1016/j.molstruc.2016.12.048>.

941 (24) Li, Z.; Cheng, C.; Zhang, L.; Xue, J.; Sun, Q.; Wang, H.; Cui, R.; Liu, R.; Song, L. Extraction  
942 of pigments from chestnut (*Castanea mollissima*) shells using green deep eutectic solvents:  
943 Optimization, HPLC-MS identification, stability, and antioxidant activities. *Food Chemistry* **2025**,  
944 *488*, 144916. DOI: <https://doi.org/10.1016/j.foodchem.2025.144916>.

945 (25) Abdollahzadeh, M.; Khosravi, M.; Hajipour Khire Masjidi, B.; Samimi Behbahan, A.;  
946 Bagherzadeh, A.; Shahkar, A.; Tat Shahdost, F. Estimating the density of deep eutectic solvents  
947 applying supervised machine learning techniques. *Scientific Reports* **2022**, *12* (1), 4954. DOI:  
948 <https://doi.org/10.1038/s41598-022-08842-5>.

949 (26) Troter, D.; Zlatkovic, M.; Đokić-Stojanović, D.; Konstantinović, S. Citric acid-based deep  
950 eutectic solvents: Physical properties and their use as cosolvents in sulphuric acid-catalysed  
951 ethanolysis of oleic acid. *Advanced technologies* **2016**, *5*, 53-65. DOI:  
952 <https://doi.org/10.5937/savteh1601053T>.

953 (27) Taysun, M. B.; Sert, E.; Atalay, F. S. Effect of Hydrogen Bond Donor on the Physical  
954 Properties of Benzyltriethylammonium Chloride Based Deep Eutectic Solvents and Their Usage  
955 in 2-Ethyl-Hexyl Acetate Synthesis as a Catalyst. *Journal of Chemical & Engineering Data* **2017**,  
956 *62* (4), 1173-1181. DOI: <https://doi.org/10.1021/acs.jced.6b00486>.

957 (28) Alshammari, O. A. O.; Almulgabsagher, G. A. A.; Ryder, K. S.; Abbott, A. P. Effect of solute  
958 polarity on extraction efficiency using deep eutectic solvents. *Green Chemistry* **2021**, *23* (14),  
959 5097-5105, 10.1039/D1GC01747K. DOI: <https://doi.org/10.1039/D1GC01747K>.

960 (29) "Glycerol.". National Library of Medicince,  
961 <https://pubchem.ncbi.nlm.nih.gov/compound/753> (accessed 2025 October 31).

962 (30) Ling, J. K. U.; Chan, Y. S.; Nandong, J. Degradation kinetics modeling of antioxidant  
963 compounds from the wastes of *Mangifera pajang* fruit in aqueous and choline chloride/ascorbic  
964 acid natural deep eutectic solvent. *Journal of Food Engineering* **2021**, *294*, 110401. DOI:  
965 <https://doi.org/10.1016/j.jfoodeng.2020.110401>.

966 (31) Vo, T. P.; Trang Nguyen, T. H.; Tran Nguyen, H. B.; Nguyen, H. N.; Nhi Le, N. V.; Ha, M.  
967 H.; Pham, G. B.; Nguyen, D. Q. Enhancing phenolic and flavonoid recovery from Vietnamese  
968 balm using green solvent-based ultrasonic-enzymatic-assisted extraction. *Ultrasonics  
969 Sonochemistry* **2025**, *121*, 107546. DOI: <https://doi.org/10.1016/j.ultsonch.2025.107546>.

970 (32) Rashid, R.; Mohd Wani, S.; Manzoor, S.; Masoodi, F. A.; Masarat Dar, M. Green extraction  
971 of bioactive compounds from apple pomace by ultrasound assisted natural deep eutectic solvent  
972 extraction: Optimisation, comparison and bioactivity. *Food Chem* **2023**, *398*, 133871. DOI:  
973 <https://doi.org/10.1016/j.foodchem.2022.133871>.

974 (33) Kaufmann, B.; Christen, P. Recent extraction techniques for natural products: microwave-  
975 assisted extraction and pressurised solvent extraction. *Phytochemical Analysis* **2002**, *13* (2), 105-  
976 113. DOI: <https://doi.org/10.1002/pca.631>.

977 (34) Zhao, M.; Li, Y.; Xu, X.; Wu, J.; Liao, X.; Chen, F. Degradation Kinetics of Malvidin-3-  
978 glucoside and Malvidin-3,5-diglucoside Exposed to Microwave Treatment. *Journal of  
979 Agricultural and Food Chemistry* **2013**, *61* (2), 373-378. DOI: <https://doi.org/10.1021/jf304410t>.



980 (35) Purbowati, I. S. M.; Maksum, A. The antioxidant activity of Roselle (*Hibiscus sabdariffa*  
981 Linii) phenolic compounds in different variations microwave-assisted extraction time and power.  
982 *IOP Conference Series: Earth and Environmental Science* **2019**, *406* (1), 012005. DOI:  
983 <https://doi.org/10.1088/1755-1315/406/1/012005>.

984 (36) Fan, Y.; Niu, Z.; Xu, C.; Yang, L.; Yang, T. Protic Ionic Liquids as Efficient Solvents in  
985 Microwave-Assisted Extraction of Rhein and Emodin from *Rheum palmatum* L. *Molecules* **2019**,  
986 *24* (15). DOI: <https://doi.org/10.3390/molecules24152770>.

987 (37) Tomasi, I. T.; Santos, S. C. R.; Boaventura, R. A. R.; Botelho, C. M. S. Optimization of  
988 microwave-assisted extraction of phenolic compounds from chestnut processing waste using  
989 response surface methodology. *Journal of Cleaner Production* **2023**, *395*, 136452. DOI:  
990 <https://doi.org/10.1016/j.jclepro.2023.136452>.

991 (38) Cao, H.; Saroglu, O.; Karadag, A.; Diaconeasa, Z.; Zoccatelli, G.; Conte-Junior, C. A.;  
992 Gonzalez-Aguilar, G. A.; Ou, J.; Bai, W.; Zamarioli, C. M.; et al. Available technologies on  
993 improving the stability of polyphenols in food processing. *Food Frontiers* **2021**, *2* (2), 109-139.  
994 DOI: <https://doi.org/10.1002/fft2.65>.

995 (39) Bener, M.; Şen, F. B.; Öнем, A. N.; Bekdeşer, B.; Çelik, S. E.; Lalikoglu, M.; Aşçı, Y. S.;  
996 Capanoglu, E.; Apak, R. Microwave-assisted extraction of antioxidant compounds from by-  
997 products of Turkish hazelnut (*Corylus avellana* L.) using natural deep eutectic solvents: Modeling,  
998 optimization and phenolic characterization. *Food Chemistry* **2022**, *385*, 132633. DOI:  
999 <https://doi.org/10.1016/j.foodchem.2022.132633>.

1000 (40) Olalere, O. A.; Gan, C.-Y. Intensification of microwave energy parameters and main effect  
1001 analysis of total phenolics recovery from *Euphorbia hirta* leaf. *Journal of Food Measurement and*  
1002 *Characterization* **2020**, *14* (2), 886-893. DOI: <https://doi.org/10.1007/s11694-019-00338-7>.

1003 (41) Vo, T. P.; Nguyen, M. T.; Ho, T. A. T.; Luong, N. L. U.; Van, L. M. U.; Nguyen, L. T. T.;  
1004 Nguyen, D. Q. Combining the natural deep eutectic solvents and high-speed-shearing-enzymatic-  
1005 assisted extraction to recover flavonoids and terpenoids from perilla leaves. *Journal of Molecular*  
1006 *Liquids* **2024**, *411*, 125720. DOI: <https://doi.org/10.1016/j.molliq.2024.125720>.

1007 (42) Vo, T. P.; Nguyen, H. N.; Pham, G. B.; La, N. A. T.; Pham, X. D. A.; Nguyen, D. Q. Application of ultrasound-microwave-assisted extraction to extract phenolic and terpenoid  
1008 compounds from celery stalk. *Journal of Agriculture and Food Research* **2025**, *24*, 102362. DOI:  
1009 <https://doi.org/10.1016/j.jafr.2025.102362>.

1010 (43) Ampofo, J.; Ngadi, M.; Ramaswamy, H. S. Elicitation kinetics of phenolics in common bean  
1011 (*Phaseolus vulgaris*) sprouts by thermal treatments. *Legume Science* **2020**, *2* (4), e56. DOI:  
1012 <https://doi.org/10.1002/leg3.56>.

1013 (44) Hobbi, P.; Okoro, O. V.; Delporte, C.; Alimoradi, H.; Podstawczyk, D.; Nie, L.; Bernaerts,  
1014 K. V.; Shavandi, A. Kinetic modelling of the solid–liquid extraction process of polyphenolic  
1015 compounds from apple pomace: influence of solvent composition and temperature. *Bioresources*  
1016 *and Bioprocessing* **2021**, *8* (1), 114. DOI: <https://doi.org/10.1186/s40643-021-00465-4>.

1017 (45) Kumar, M.; Tomar, M.; Punia, S.; Amarowicz, R.; Kaur, C. Evaluation of Cellulolytic  
1018 Enzyme-Assisted Microwave Extraction of *Punica granatum* Peel Phenolics and Antioxidant  
1019 Activity. *Plant Foods for Human Nutrition* **2020**, *75* (4), 614-620. DOI:  
1020 <https://doi.org/10.1007/s11130-020-00859-3>.

1021

1022



## Data availability statements

Data will be made available on request..

